Nerve GPS: A decision support system for the identification of neural components in ultrasound-guided nerve block

Christophe Philippona

Masters of Science in Experimental Surgery

Department of Surgery

Division of Experimental Surgery

Faculty of Medicine

McGill University

Montreal, Quebec, Canada

May 14, 2014

A Thesis submitted to the Faculty of Graduate and Postdoctoral Studies in partial fulfillment of the requirements for the degree of Master of Science

DEDICATION

This document is dedicated to the graduate students of the McGill University.

ACKNOWLEDGMENTS

I thank the graduate students of the Intelligent Technology in Anaesthesia Group (ITAG) lab for their support throughout the project.

Fellow master's student Joshua Morse was more than helpful in the learning and development of the thesis. Without the help he provided in several stages of development, testing and editing among others, the project would likely not have yielded the same positive results.

Doctoral student Mohamad Wehbe was valuable in providing advice from his own experience working in clinical studies and biomedical engineering for several years. The advice he provided helped build the pillars on which this project was based.

I also thank the other members of the ITAG lab – Marilu Giacalone & Shantale Cyr – for their participation and support during studies involving the NerveGPS. In addition I would like to thank Shantale Cyr for providing help in study coordination and the references she provided for personal grants obtained during the course of the master's.

***

Most importantly, I would like to thank Dr. Thomas Hemmerling for the opportunities, direction, advice, knowledge and support he provided and has offered to provide throughout the course of the master's project and future endeavours. Without the direction and insight provided by Dr. Hemmerling, this project could not have taken form. I owe Dr. Hemmerling my success in my graduate studies and initial pursuit of my professional goals.

TABLE OF CONTENTS

DEDICATION ii
TABLE OF CONTENTS iv
LIST OF TABLES vi
LIST OF FIGURES vii
- Chapter 1 – Introduction 1
  1. 1. Introduction 1
  1. 2. Objectives of the project 3
  1. 3. Research hypotheses 3
- Chapter 2 – Background & Literature Review 5
  2.1. Anaesthesia 5
  2.1. Ultrasound-Guided regional nerve blockade 6
    2.1.1. Ultrasound-Guided Sciatic nerve block at the popliteal fossa 6
    2.1.2. Ultrasound-Guided Femoral nerve block 9
  2.2. Evolution of regional nerve blockade 10
    2. 2. 1. Peripheral Nerve Stimulation 10
    2. 2. 2. Ultrasound Guided nerve blockade 11
    2. 2. 3. Advantage of ultrasound-guided over peripheral nerve stimulation 11
  2. 3. Ultrasound imaging technology 12
    2. 3. 1. Existing ultrasound platforms 13
    2. 3. 2. Ultrasound image filtering 15
    2. 3. 3. Ultrasound for medical diagnostics 16
    2. 3. 4. Image enhancement technology in interventional ultrasound 18
- Chapter 3 – NerveGPS: Decision Support System 21
  3. 1. Organizational flowchart for nerve detection 21
    3. 1. 1. Sciatic nerve at the popliteal fossa 21
    3. 1. 2. Femoral Nerve 24
  3. 2. Graphical User Interface 27
    3. 2. 1. Principles of Graphical User Interfaces (GUI) 27
    3. 2. 2. Presenting the graphical user interface 29
  3. 3. User feedback 34
- Chapter 4 – Nerve detection algorithm 35
  4. 1. Overview 35
  4. 2. Image acquisition 36
  4. 3. Filter 37
    4. 3. 1. Speckle noise filtering 37
    4. 3. 2. Black box testing 38
  4. 4. Histogram matching 40
  4. 4. Image segmentation 42
    4. 4. 1. K-means 42
    4. 5. Scoring 43
    4. 5. 1. Data collection 45
    4. 5. 2. Determining weights 49
    4. 5. 3. Edge cases and extrema settings 51
    4. 6. Active Contours 53
  4. 7. Final Score 55
- Chapter 5 – Testing & Results 58
  5. 1. Study setup 58

5. 1. 1. Study Design 59
5. 1. 1. 1. Protocol 60
5. 1. 1. 2. Evaluation of results 62
5. 1. 1. 3. Analysis 64
5. 1. 2. Results 64
5. 1. 2. 1. Part I results: Image analysis 64
5. 1. 2. 2. Part II results: Video Analysis 66
5. 2. Part III results: Decision support testing 68
• Chapter 6 – Discussion 70
6. 1. Discussion 70
6. 2. Future Work 76
6. 2. 1. Robotic applications 77
6. 2. 2. Robotics in medicine and anaesthesia 78
Chapter 7 – Conclusion 81
Appendix 1 – IEEE proceeding: "Nerve GPS: A novel decision support system for ultrasound nerve block guidance" 83
Abstract 83
I. INTRODUCTION 84
II. BACKGROUND 85
A. Ultrasound 85
B. Nerve block 86
III. METHODS 87
A. Setup 87
B. Filtering methods 87
C. Evaluation of results 89
IV. DISCUSSION 89
LIST OF REFERENCES 95

LIST OF TABLES

Table 1: Weight distribution for each descriptor 50
Table 2: Breakdown of scores with individual weights for the objects seen in Figure 27 57
Table 3: Average nerve detection overlap for the sciatic nerve at the popliteal fossa 65
Table 4: Average nerve detection overlap for the femoral nerve...66
Table 5: Video detection results for the sciatic nerve at the popliteal fossa on 6 subjects. 67
Table 6: Video detection results for the femoral nerve...68
Table 7: Results of NerveGPS use for the sciatic nerve at the popliteal fossa.........................69
Table 8: Results of NerveGPS use for the femoral nerve 69

LIST OF FIGURES

Fig. 1: Probe placement for the start of ultrasound guided sciatic nerve block using a traceback approach (posterior) with the patient in a prone position......................................7
Fig. 2: Annotated landmarks of the popliteal anatomy on sample participant........................8
Fig. 3: Anatomical view of the area surrounding the sciatic nerve at the popliteal fossa. Adapted from (H. Gray, 1918). 8
Fig. 4: Probe placement for ultrasound-guided femoral nerve block. Adapted from (Anesthesia, 2013)...9
Fig. 5: Anatomical considerations for the femoral nerve (right) and example sonoanatomy (left). Adapted from (Anesthesia, 2013)...10
Fig. 6: Sonosite X-Porte ultrasound platform (Sonosite, 2013) 14
Fig. 7: Flowchart for popliteal nerve detection 22
Fig. 8: Steps for detection of sciatic nerve at the popliteal fossa...23
Fig. 9: Flowchart for femoral nerve detection..24
Fig. 10: Steps for detection of femoral nerve 26
Fig. 11: NerveGPS UI panel with instructions for Step 2..30
Fig. 12: Presentation of the NerveGPS UI panel...31
Fig. 14: Overview of the sciatic nerve detection image-processing flowchart 36
Fig. 15: Image acquisition flowchart...37
Fig. 16: MATLAB's wavelet toolbox being used for an ultrasound image..............................40
Fig. 17: Histogram matching results on an image of the popliteal nerve. Figures a) & c) are the original image and its intensity histogram respectively and figures b) & d) are the resulting image and its histogram respectively. 41
Fig. 18: a) and b) represent the images before and after k-means respectively. At bottom, binary images representing each intensity cluster. Illustration of results of k-means for image segmentation of sciatic nerve ultrasound image. 43
Fig. 20: Graph representing the eccentricity/compactness distribution of all objects (blue) and those that correspond to nerves (red). The graph is a frequency plot representing the eccentricity/compactness regional descriptor of all objects (blue bars) compared to that of the nerves (red bars). 47
Fig. 21: Frequency plot representing the extent regional descriptor of all objects (blue bars) compared to that of the nerves (red bars). 48
Fig. 22: Frequency plots representing the intensity regional descriptor of all objects (blue bars) compared to that of the nerves (red bars)..49
Fig. 23: Frequency plots representing the height-to-width regional descriptor of all objects (blue bars) compared to that of the nerves (red bars)..49
Fig. 24: Graph illustrating the mapping of values to scores for the intensity regional descriptor. The y-axis represents the score before weighting (this score can have a maximum of 1) and the x-axis represents the value of the intensities between 0 and 255. 51
Fig. 25: Region boundaries set by anatomical landmarks on an ultrasound image in the sciatic region: skin & fascia at top and vessels at bottom...53
Fig. 26: Illustration of active contours. Figure a) shows the k-means segmented image with the object determined as the nerve shaded in red and the red bounding box used to grow the contour. Figure b) shows the result of the active contour growing 54
Fig. 27: Ultrasound image of the sciatic nerve, annotated to show location of objects most likely to be the nerve. Figure a) shows the image segmentation output and Figure b) shows the centroids of the objects most likely to be the nerve. (cf. Table 2). Figure a) shows the output of the k-means algorithm to illustrate the objects that the stars correspond to in

Figure b). In Figure b) we can see the center of the 3 objects provided by the voting algorithm. The red star marked as 1 corresponds to the most likely object with the highest score (89) as can be seen in Table 2. 56
Fig. 28: Setup for the study....59
Fig. 29: Illustration of probe placement and movement for ultrasound nerve block. The arrow shows the direction of probe movement during the study. The picture in picture (top right) represents the display of the ultrasound with the probe in this position....61
Fig. 30: Illustration of evaluation methods. The center point of the concentric circles corresponds to the software detected nerve center and the red contour corresponds to the manually detected nerve area. 63
Fig. 31: Illustration of overlap evaluation method....64
Fig. 32: Ultrasound probe placed on an ultrasound nerve block training phantom (BluePhantom, 2013)....71
Fig. 33: Ultrasound image obtained by placing an ultrasound probe on the ultrasound nerve block training model as seen in Figure 32. (BluePhantom, 2013)....72
Fig. 34: Limitations of the evaluation method used to determine overlap between the manual and automated nerve detections....74
Fig. 35: Views of the Magellan robot assisted ultrasound-guided nerve block (Thomas M Hemmerling et al., 2013). In a) a view of the arm being used on a patient and b) the cockpit view....78

ABSTRACT

Objective – The objective of this project was the development of a decision support system for ultrasound guided nerve block with a built in automated nerve detection software.

Method – The decision support system consists of a graphical user interface that provides the user with instructions for manipulating the ultrasound probe to find the region of interest for nerve block. Once located, the user can chose to use the automated detection software to locate the nerve. The automated detection software uses a 6-step image processing algorithm to locate the nerve: 1) filtering, 2) histogram matching, 3) k-means segmentation, 4) feature extraction using regional descriptors, 5) scoring and 6) Chan-Vese active contour extraction. The system was developed for the sciatic nerve at the popliteal fossa and the femoral nerve.

Results – The algorithm was tested on still images and videos. Still images yielded very positive results: 100% and 83% successful detections for the popliteal nerve (100 images) and femoral nerve (120 images) respectively, with a 98% and 83% overlap between the software's detection and an anaesthesiologist's for a circle of 0.4cm from the nerve center. Video testing (10 videos of ~300s in length) yielded equally positive results and a runtime of 451ms for the algorithm. Tests performed to validate the protocol provided by the decision support systems were 75% successful for the popliteal nerve (3/4) and 100% successful for the femoral nerve (4/4).

Discussion – In this pilot study of the ultrasound guided decision support system, the results showed that such an application was feasible. The system, including the nerve detection software, could be used for ultrasound specialty training or to provide the clinician with a second opinion during nerve block.

A. ABRÉGÉ

Objectif – L'objectif de ce projet est de réaliser un outil d'aide à la décision pour les blocs nerveux échoguidés avec un logiciel permettant l'identification du nerf à partir de l'image échographique fournie.

Méthodes – L'outil d'aide à la décision est constitué d'une interface graphique fournissant les instructions nécessaires à l'utilisateur pour permettre de placer la sonde échographique dans la région souhaitée. Une fois le nerf identifié, l'utilisateur a l'option d'activer le détecteur automatique du nerf. Le logiciel de détection du nerf se divise en un algorithme de traitement d'image séquencé en 6 étapes : 1) filtre, 2) normalisation du contraste, 3) segmentation k-means, 4) extraction de caractéristiques morphologiques, 5) classement et 6) contour. Le système a été développé pour le nerf sciatique dans la fosse poplitée et le nerf fémoral.

Résultats – L'algorithme a été testé sur des images fixes et des vidéos. Des résultats prometteurs ont été obtenus pour les images fixes : 100% d'identifications réussies pour le nerf sciatique (100 images) et 83% pour le nerf fémoral (120 images), avec un chevauchement de 98% et 83% entre l'aire de l'identification du logiciel et celui d'un anesthésiste pour un cercle de 0.4cm de diamètre avec pour centre le centre du nerf. Les résultats de l'évaluation vidéo (10 vidéos d'environ 300s) ont aussi été très positifs et ont permis de mesurer la performance de l'algorithme a 451ms. Les tests pour valider l'outil d'aide à la décision ont donné 75% de réussite pour le nerf sciatique (3/4) et 100% de réussite pour le nerf fémoral (4/4).

Discussion – Dans cette étude, la faisabilité d'un outil d'aide à la décision pour les blocs nerveux échoguidés a été démontrée. Le système, qui inclut un algorithme de détection automatique du nerf pourra aider à la formation.

• Chapter 1 – Introduction

1. 1. Introduction

Ultrasound guided nerve blockade is a procedure used in regional anaesthesia that requires excellent technical skills that sometimes requires an additional fellowship to acquire expertise (Hargett, Beckman, Liguori, & Neal, 2005). The two techniques most commonly used for peripheral nerve blockade today are peripheral nerve stimulation and ultrasound guidance. Prior to this, nerve blocks were performed using anatomical landmarks and paresthesia. Ultrasound guidance offers a safer procedure with a higher success rate than peripheral nerve stimulation. Reports indicate that success rates in performing ultrasound guided nerve blocks are of around 89% as opposed to 70% for peripheral nerve stimulation (V. S. Chan et al., 2007). The full penetration of ultrasound is hindered by the cost of the procedure. Ultrasound guided nerve block is different from other regional anaesthesia procedures and it is believed that the procedure would benefit from its own training program (Chin & Chan, 2008). Even among trained anaesthesiologists, obtaining consistent and interpretable images is difficult and requires a good knowledge of the sonoanatomy and technical skills in handling the probe and adjusting the angles for the best visibility (Sinha & Chan, 2004). To improve patient safety and support the higher reliability of a successful procedure, a decision support system could be developed to help remove some of the complex and operator dependent aspects of the ultrasound guided procedure.

A decision support system supplements the usual training tools used. A decision support system could also help clinicians in an interventional setting. Anaesthesiologists perform interventional procedures on the body, which requires clinicians to have a very good knowledge of anatomy (Bodenham, 2006). A decision support system could thus help the clinician and improve patient safety and ensure successful procedure completion.

There are 2 main parts to ultrasound guided regional nerve blockade: 1) localization of the nerve and 2) insertion of the block needle. Current works aim at improving the accessibility and reducing the complexity of ultrasound-guided nerve blocks. These works have focused mostly on improving needle visualization within the ultrasound image or developing needle insertion aids (Shi, Schwaiger, & Lueth, 2011). Few studies have looked into improving nerve visualization outside of general ultrasound filtering. Nerve visualization is not always obvious however: 87% of sciatic nerves were not detected in a study by Chan et al (V. W. Chan, Nova, Abbas, McCartney, & Perlas, 2006).

To improve nerve visualization, nerve detection software could be developed. When activated, this software would overlay the position of the nerve on the ultrasound feed. The behaviour and use case for this software would be analogous to that of the color Doppler widely used as an essential diagnostic tool in certain procedures. This paper will detail the steps taken to develop this system and the results obtained.

1. 2. Objectives of the project

The objective of this project is the development of automated nerve detection software for use in a decision support system for ultrasound-guided nerve block. The software will use image processing techniques to identify the nerve within images obtained from an ultrasound platform and guide the physician through the steps of performing a nerve block.

The project is thus divided into 3 parts:

1. Development of a user interface to guide the physician through the project.
2. Development of independent solutions for identifying the nerves within ultrasound images.
3. Interfacing with the future robotic and mechanical and robotic components of the system.

1. 3. Research hypotheses

We are capable of developing software for the automated detection of the following nerves:

- Femoral nerve
- Sciatic nerve at the popliteal fossa.

The automated detection software will be integrated into the decision support system.

Detection of the landmarks for nerve block is done using ultrasound and the user follows the protocol proposed by the decision support system software.

The software is used as a “second opinion” and does not constitute the sole basis for detection of the nerve.

• Chapter 2 – Background & Literature Review

This section will outline the current technologies that exist and the need for the system that is being developed.

2.1. Anaesthesia

Anaesthesia is a temporary drug induced loss of sensation in a part or the body. Anaesthesia allows for preoperative, intraoperative and postoperative pain suppression. There are three main types of anaesthesia: general anaesthesia, regional anaesthesia and Monitored Anaesthesia Care. General anaesthesia features three principal components: analgesia, hypnosis and neuromuscular blockade. These components affect the patient's entire body, making it harmful and dangerous for patients in certain conditions or after certain types of trauma. To avoid and prevent the dangers of general anaesthesia, the anaesthesiologists will often opt for regional anaesthesia in cases that do not require general anaesthesia. For regional anaesthesia the anaesthesiologists will only focus on the suppression of pain from the region of interest in the patient's body. In addition, it also features a cost advantage over general anaesthesia when the surgery or post-operative pain management is limited to a specific region of the body. There are several ways in which to administer regional anaesthesia. This paper will focus on the regional nerve blockade.

2.1. Ultrasound-Guided regional nerve blockade

The ultrasound guided nerve blockade procedure is specific to the area of the body being anesthetised. In this subsection we will present the procedures used for the sciatic nerve at the popliteal fossa and the femoral nerve.

2.1.1. Ultrasound-Guided Sciatic nerve block at the popliteal fossa

The sciatic nerve block at the popliteal fossa is used when performing surgery or postoperative pain management on the calf, Achilles tendon, ankle or foot (Vloka, Hadžic, April, & Thys, 2001; Vloka et al., 1996). To perform the nerve block, the patient can be placed in the prone or supine position and occasionally on their side. Two approaches can be used: posterior – the probe is placed at the popliteal crease – and lateral – the probe is placed to the side of the patient's leg. The traceback approach is used with the patient in the prone or supine position while employing a posterior approach. To perform the traceback approach, the probe is placed at the popliteal crease to first visualize and locate the artery (Figure 1). The anaesthesiologist then moves the probe cranially following the vessel, in an attempt to locate landmarks. The first landmarks (Figure 2) are the tibial and common peroneal nerves. The nerves can be located due to 3 characteristics: their oval shape, their hyperechoicity and their position lateral to the artery. The anaesthesiologist then moves the probe cranially until the two aforementioned nerves merge together into the sciatic nerve (Figure 3). The bifurcation usually occurs 5-12 cm above the popliteal crease. The clinician then inserts the anaesthetic around the nerve (Bigeleisen, 2006; Borgeat,

2006) until the displacement of the nerve and tissue can be seen in the ultrasound feed.

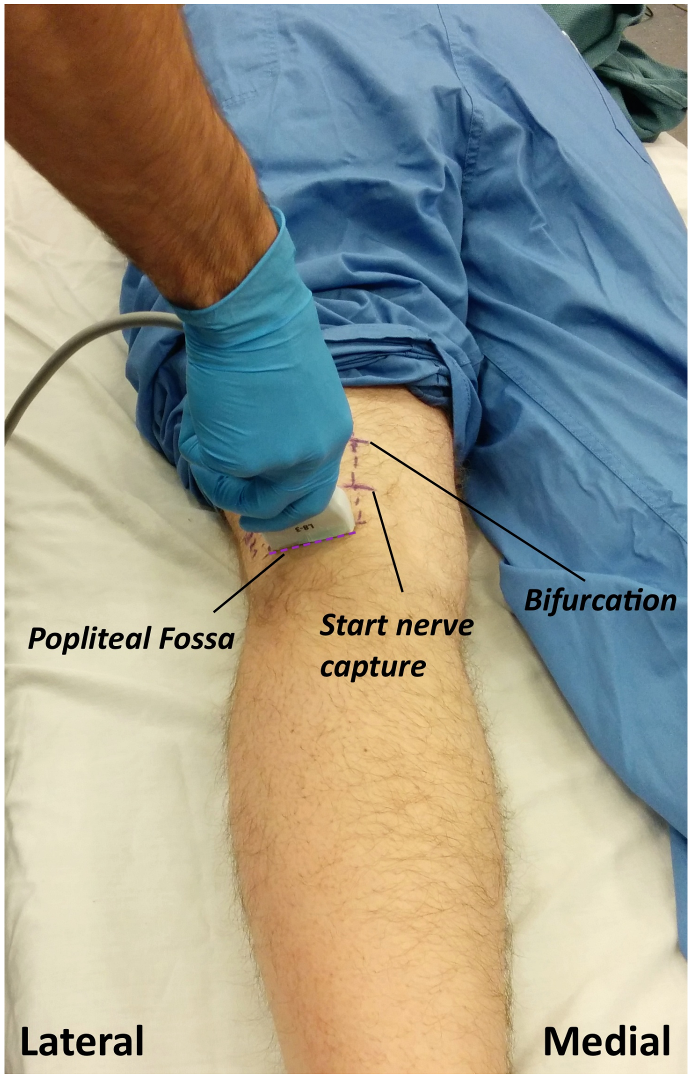

Fig. 1: Probe placement for the start of ultrasound guided sciatic nerve block using a traceback approach (posterior) with the patient in a prone position

The same procedure applies when the patient is in a supine position.

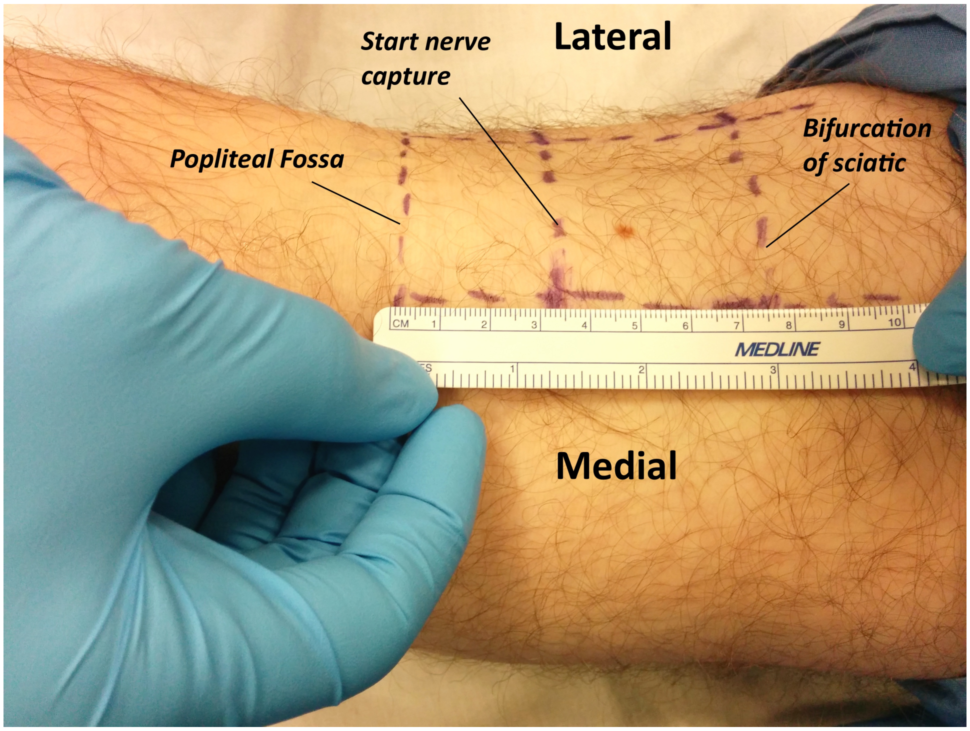

Fig. 2: Annotated landmarks of the popliteal anatomy on sample participant

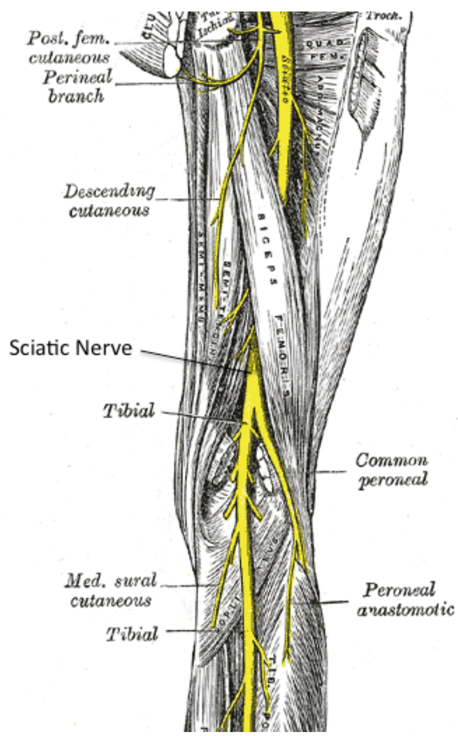

Fig. 3: Anatomical view of the area surrounding the sciatic nerve at the popliteal fossa. Adapted from (H. Gray, 1918).

2.1.2. Ultrasound-Guided Femoral nerve block

Ultrasound guided femoral nerve block is used when performing surgery on the anterior thigh, knee or femur. To perform the block, the patient is placed in a supine position. The transducer is placed in a transverse position at the inguinal crease (Figure 4) to locate the femoral artery, which is easily identifiable at this level.

Fig. 4: Probe placement for ultrasound-guided femoral nerve block. Adapted from (Anesthesia, 2013)

Once the probe is placed, the user moves the probe laterally and medially to the artery. The nerve can then be found using an ultrasound depth of 2-4cm immediately lateral to the femoral artery, below the fascia iliaca (Figure 5). Its sonoanatomy characteristics are its hyperechoicity and triangular or oval shape. After identification, the needle and the local anaesthetic is inserted near the nerve (Anesthesia, 2013).

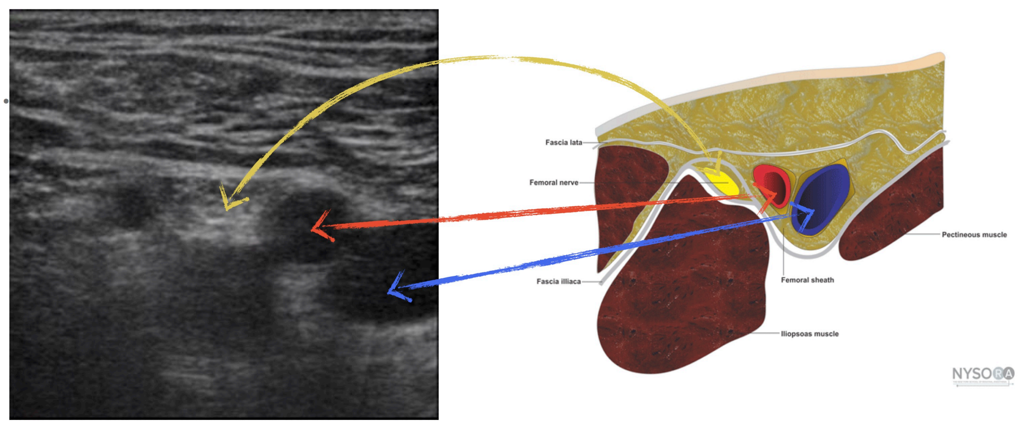

Fig. 5: Anatomical considerations for the femoral nerve (right) and example sonoanatomy (left). Adapted from (Anesthesia, 2013)

2.2. Evolution of regional nerve blockade

2. 2. 1. Peripheral Nerve Stimulation

Regional nerve blockade can be performed using peripheral nerve stimulation. For peripheral nerve stimulation, the anaesthesiologist delineates the needle insertion site by identifying anatomical landmarks. Once the anatomical landmarks have been identified, the anaesthesiologist will insert a needle to which a small current around 0.5mA is introduced into the region of interest. The anaesthesiologist then confirms the location of the nerve by a physiological response to the applied current in the form of a muscle twitch. Once the correct location of the nerve is confirmed, they inject the anaesthetic and verify the successful action of the anaesthetic.

2. 2. 2. Ultrasound Guided nerve blockade

Ultrasound-guided regional nerve blockade is a more recent technique for regional anaesthesia. The clinician uses an ultrasound platform and an ultrasound transducer at the region of interest. The clinician sweeps the area and identifies the anatomical landmarks of the patient's sonoanatomy. Once confident with the interpretation of the sonoanatomy, the needle can be inserted using an in plane or out of plane approach. The anaesthesiologist tracks the advancement of the needle using the ultrasound machine. When satisfied with the location of the needle, the anaesthesiologist follows the spread and effects of the anaesthetic as it is injected near the nerve.

2. 2. 3. Advantage of ultrasound-guided over peripheral nerve stimulation

Ultrasound-guided regional nerve blockade has several advantages over the peripheral nerve stimulation technique. Ultrasound gives the clinician a view of the patient's sonoanatomy and a precise spatial indication of all anatomical landmarks. The added visibility gives the clinician the ability interpret and adapt to difficult or unfamiliar anatomies. The procedure becomes safer and more reliable as well (A. T. Gray, 2006; Kapral et al., 2008; P Marhofer, Sitzwohl, Greher, & Kapral, 2004; Perlas et al., 2008; Sandhu & Capan, 2002). When guiding the needle for injection of the anaesthetic, knowledge of the precise location of important anatomical elements can reduce the risk of adverse events such as vascular puncture. When injecting the anaesthetic, the anaesthesiologist can follow its spread on the ultrasound machine and judge its effects. With the success of the first injection, the volume of anaesthetic used can be decreased. Decreasing the volume of anaesthetic decreases the risk of drug toxicity cause by administration of excessive volumes of anaesthetic (Neal, 2010). Finally, ultrasound-guidance is less invasive than peripheral nerve stimulation. Studies have shown that ultrasound-guidance reduces the number of needle insertions performed to inject the anaesthetic (Koscielniak-Nielsen, 2008). Removing electrical stimulation of the nerves eliminates discomfort that may be experienced by the patient. In addition, ultrasound-guided nerve blocks prevent complications that may arise in trauma regions due to muscle twitches caused by the electrical stimulation of the nerve (Koscielniak-Nielsen, 2008).

2. 3. Ultrasound imaging technology

Imaging technology plays a critical role in medicine. It allows doctors to obtain information about the patient that may not be immediately apparent in tests and visual observation. Imaging technology can be used for procedural tasks and diagnostics. Clinicians select the most appropriate by considering many factors including cost, invasiveness and how well suited it is to the given application. Ultrasound imaging technology presents many advantages over other imaging that make it the ideal tool in many applications. Ultrasound imaging allows clinicians to view the location, shape and size of many internal organs including muscles, nerves and ligaments and does so with minimal invasiveness, posing no currently known risks to the patient (Hangiandreou, 2003). Ultrasound imaging allows real-time visualization of images, and is more portable and cost-effective than other imaging alternatives: magnetic resonance imaging (MRI), X-Ray and computed tomography (CT). Due to all these advantages, ultrasound is becoming more prevalent across health disciplines. To benefit fully from all the advantages that ultrasound imaging has to offer, a wide body of research has emerged to improve its use. The research being done in ultrasound imaging can be classified in 3 different categories:

1. Ultrasound image filtering
2. Techniques to improve or perform diagnostic ultrasound
3. Techniques to improve or perform interventional ultrasound

The following paragraphs present some of the research that has been done in these fields.

2. 3. 1. Existing ultrasound platforms

The Zonare z.one ultrasound platform was used for studies and development due to its availability to the authors of the study. The ultrasound platforms available to the authors of the study at the McGill University Health Centre (MUHC) were developed by Sonosite (Bothell, WA, USA), Zonare (Mountain View, CA, USA), Philips (Amsterdam, NL) and General Electric (Fairfield, CT). These platforms are developed for several applications in medicine and the design of each is dependent on the use case it was intended for. The use of ultrasound machines is contingent on their suitability for the use case (correct probes), the quality of the image and the ease of use. The quality of the ultrasound image, which determines how easy an image may be to interpret, varies from one ultrasound platform to another, depending on the noise filtering methods used.

Newer generations of ultrasound machines provide the user with more functions, increased ease of use and an increasingly integrated process. Many of the improvements come in the touchscreen user interfaces, which make the systems both more intuitive and less cumbersome. Among the newer platforms, the Sonosite X-Porte (Figure 6) stands out thanks to its onboard tutorials. The Sonosite X-Porte features 2 touchscreens, one for the display of the ultrasound feed and another that allows the user to pull up tutorials that may serve as refreshers when performing a less common procedure. This second screen opens the door for easier integration of ultrasound based decision support systems in the operating room.

Fig. 6: Sonosite X-Porte ultrasound platform (Sonosite, 2013)

2. 3. 2. Ultrasound image filtering

Ultrasound imaging in medicine uses ultrasound waves between 5MHz and 14Mhz to visualize elements inside the body (P. Marhofer, Greher, & Kapral, 2005). The frequency of the ultrasound waves determines the depth of penetration of the ultrasound wave, which in turn determines the depth of analysis. Low frequencies have a higher penetration depth than high frequencies. The depth of analysis is important and dependent on the operation. Frequencies also determine the resolution of the image. Lower frequencies offer a high depth of penetration but offer a lower resolution. When performing procedures that require the visualization of superficial elements a higher frequency is used for a better resolution, however lower frequencies are favoured for more profound structures. The frequency of the ultrasound waves is chosen at the start of procedures.

The probe sends the waves into the region of interest. As the waves hit structures in the body, they are reflected at different intensities, angles and times. The ultrasound probe picks up the waves that were reflected in its direction and the ultrasound platform analyzes them to build the ultrasound image. Muscles, vessels, ligaments and other body structures are more easily distinguishable in ultrasound images.

Distinguishing these structures is complicated by speckle noise. Speckle noise is a random interference pattern that results from stray or low intensity ultrasound waves that increases the difficulty of interpretation. Due to the importance of a clear image for interpretation, there exists a large body of research on the reduction of ultrasound speckle noise.

In 2 studies by Portnoy & Milgram (Portnoy & Milgram, 2008; Portnoy, Milgram, & McCartney, 2008), the authors propose a filter that would increase the saliency of the peripheral nerve image and thus contribute to the increase in the usage, and adoption of peripheral nerve block techniques. A low-pass persistence filter was applied to a set of images. This filter uses the concept of trailing frames, whereby the current frame is composed of a certain amount of past and present frames. The consistent elements in these frames are considered to be the desired anatomical structures and are thus given a more important weighting. Other elements are considered random-pattern speckle noise. With an increasing amount of trailing frames, the signal to noise ratio is increased and the structures of interest more directly visible to the operator. 24 participants were asked to analyze simulated ultrasound images containing a target that was either static or moving. The study found that the participants were able to identify the targets easier with the filter. The authors propose extending this filter to real ultrasound images to facilitate sonoanatomy interpretation during ultrasound guided nerve block.

2. 3. 3. Ultrasound for medical diagnostics

Ultrasound imaging is increasingly used to diagnose lesions, tumors and other conditions in medicine. Ultrasound offers convenient means to detect these conditions. The diagnosis is often complicated when anatomical signs of these conditions are either very small or appear in a non-distinct shape that is difficult to interpret. Research in medical ultrasound is aimed at improving the diagnostic process and the tools available.

Computers and technology are used to assist in detecting lesions in ultrasound diagnostics. Ruggiero et al. (Ruggiero et al., 1998) developed a program to classify lesions automatically and recognize malignant ones. The goal of the system was to create a decision support system that provided knowledge based and automatic recognition tools. The authors used artificial neural networks, training on texture and shape indicators. The study was performed with 41 carcinoma (malignant solid lesions), 41 fibroadenoma and 41 cyst. The parameters used for neural network training were based on those used by clinicians for diagnosis. Shape parameters included radial distance from the centroid of the lesion, depth, width, depth-width ratio and correlation dimension. The neural network was a 3-layer backpropagation neural network using the MATLAB environment toolbox. The authors concluded that it was not possible to separate all 3 types using this neural network, likely due to the limited dataset available. In this case, shape classification proved more useful than texture classification for detection of carcinomas. Using a larger dataset and expanding the number of parameters used for classification could likely improve the results of the study.

The importance of automation in improving ultrasound diagnostics was highlighted in a recent review of techniques used for automated detection and classification of breast cancer (Cheng, Shan, Ju, Guo, & Zhang, 2010). The applications all use a standard approach to object detection: pre-processing, segmentation, feature extraction and classification. The need for automated breast cancer detection programs is born out of the superiority of the diagnostic technique over mammography in the successful detection of lesions. Pre-processing is divided into speckle reduction and image enhancement. For speckle reduction, the studies use a filtering technique, a wavelet approach or a compounding approach. Each method has its advantages and disadvantage in terms of development, time and resource complexity. For segmentation, the computer aided diagnostic systems use histogram thresholding, active contour models, Markov random field models or neural networks. Histogram thresholding is easy to implement and fast however unsuited for non-bimodal histograms. Active contour models can extract the lesion boundary and shape however the iterative process is detrimental to the algorithms runtime. Neural networks are the most commonly used method in ultrasound image segmentation. Given a set of inputs, these networks act as a classification tool. The success of these operations is dependent on the dataset - which must be sufficiently large to provide an accurate answer after training - and the training set - which must be representative of the lesions that can or will occur. During feature extraction, algorithms analyze features that are divided into 3 main categories: texture, shape and regional parameters and descriptor. Descriptor features refer to the elements that are characteristic of the lesions and those that set them apart. For final classifications of the lesions, some studies opt for classification based on the proximity of the extracted features to a set of rules for each group. Other designs include neural networks, which offer the best accuracy with the proper training set, template matching and decision trees. The number of techniques possible for image processing of ultrasound images and their permutations make finding the right technique to analyze the image a challenge. There is no standard technique that can be used; a decision must be made on the technique most suited for the use case.

2. 3. 4. Image enhancement technology in interventional ultrasound

Image enhancement technology removes operator dependency in interventional ultrasound. The systems being developed mainly focus on needle visualization in ultrasound. In regional nerve blockade, once the nerve has been located, the anaesthesiologist will insert the needle and try and guide it to the identified target using the ultrasound. Although in-plane and out-of-plane tracking of the needle remains a complicated task (Brian D Sites, John D Gallagher, Joseph Cravero, Johan Lundberg, & George Blike, 2004). Varying the orientation of the needle and needle bevel with relation to the probe has been shown to enhance the visibility of the needle however it may come at the cost of operator comfort or loss of other information (Schafhalter-Zoppoth, McCulloch, & Gray, 2004). To solve this problem, alternative tools such as the SonixGPS (Ultrasonix, Richmond, British Columbia, Canada) aid the clinician in predicting the trajectory and final destination of the needle (Choquet, Abbal, & Capdevila, 2013). Needle visibility can also be enhanced by using echogenic needles that feature an echogenic coating and dimpled shaft to improve echoicity. These needles are not extensively tested for nerve blocks and may not always yield a significant increase in visibility (Chin, Perlas, Chan, & Brull, 2008). Other solutions have been proposed to enhance the visibility of the needle within the ultrasound image.

A solution for needle tracking was proposed by C. Chan et al. (C. Chan, Lam, & Rohling, 2005). The authors of this study created a device that would measure the position of the needle with respect to the ultrasound probe. The system uses cameras to calculate the angle and orientation of the needle and project it onto the ultrasound screen. Alternatively, another study employs Acoustic Radiation Force Impulse Imaging for needle visualization (Rotemberg et al., 2011). This group uses another imaging technique ARFI, which allows for better needle visualization. The ARFI image is segmented to identify the needle and overlay its position onto the paired ultrasound B-mode image. Using this technique the group was able to visualize the needle tip within 2mm of its actual location in all images, confirming the feasibility of the technique.

Needle visualization is an essential component of nerve block that remains difficult even for experienced anaesthesiologists. The techniques developed to enhance visualization focus on combining image processing and other methods for a better result. Other technologies are using similar techniques to improve the use of ultrasound in diagnostics and interventions.

• Chapter 3 – NerveGPS: Decision Support System

Decision support systems in medicine provide physicians with a support tool to facilitate and consolidate the decision making process. The NerveGPS training tool is intended as an on-board educational tool providing the clinician with a step-by-step approach to the procedure.

3. 1. Organizational flowchart for nerve detection

The aim of the decision support system is to break the ultrasound guided nerve block procedure into discrete steps from setup to needle insertion. The decision support system also integrates the automated nerve recognition algorithm in an intuitive manner to help the clinician in the procedure. The technique and approach to a nerve block however is different depending on the area of the body being anesthetised. This section will present the approaches chosen for the popliteal and femoral nerves in the NerveGPS.

3. 1. 1. Sciatic nerve at the popliteal fossa

The proposed decision-support system's approach for a sciatic nerve ultrasound-guided nerve block at the popliteal fossa is posterior. The posterior approach can be used with the patient in a prone or oblique position with their legs slightly abducted (NYSORA, 2013). An anesthesiologist adapted the protocol provided for the nerve block from the guidelines set forth in the literature. The flowchart given by the NerveGPS software can be seen in Fig. 7 and a detailed description of the steps and the accompanying support instructions are collected in Fig. 8. Steps 1 and 2 guide the user through the setup of the ultrasound platform and the ultrasound transducer placement. Step 3 guides the user through the movement of the probe and the identification of vessels using Doppler. In step 4 the user activates the automated nerve detection. In step 5, if there is agreement between the detection and the anesthesiologist, the clinician should perform the nerve block, otherwise they should move the probe as recommended in step 6 before returning to step 4.

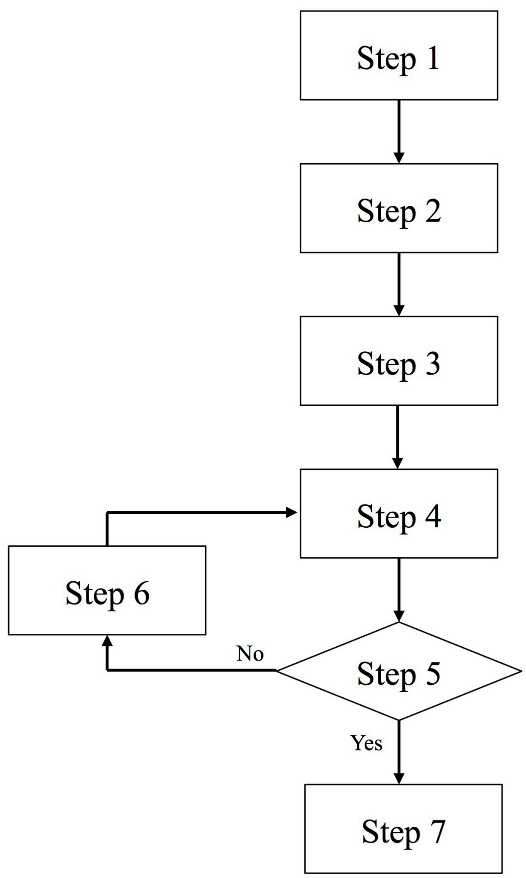

Fig. 7: Flowchart for popliteal nerve detection

	Instructions	Prompt	Picture Display
Step 1	Probe: Linear array transducer Frequency: 8-12 MHz Depth: - 5cm standard patient - 6cm obese patient	Action: Press `'Enter'`	Probe
Step 2	Place transducer perpendicular to the skin in a transverse orientation at the popliteal artery. Turn on color Doppler.	Action: Press `'Locate Artery'` or `'Enter'`	Probe
Step 3	Move probe cranially by 3.5cm to 4cm. Turn off color Doppler.	Action: Press `'Capture Nerve'` or `'Enter'`	Leg with markings and fade into probe and end with sonoanatomy
Step 4	Keep probe still until progress bar is full. Red Circle: Most probable nerve location. Heat map: History of the hits for the program	Action: Wait for progress bar.	Heat map
Step 5	If location is confirmed, perform nerve block, else move probe cranially by 1.5cm to 2 cm.	Action: Press `'Confirm'` or `'Continue Detection'`	Heat map
Step 6	Move probe cranially by 0.5cm to 1cm. As you advance cranially you should approach the bifurcation of the sciatic nerve into the tibial and peroneus nerves	Action: Press `'Capture Nerve'` or `'Enter'`	Leg with markings and fade into probe and end with sonoanatomy
Step 7	Insert Needle	Action: Insert needle	

Fig. 8: Steps for detection of sciatic nerve at the popliteal fossa

3. 1. 2. Femoral Nerve

For the ultrasound-guided nerve block of the femoral nerve, the decision support system proposes a frontal approach. The patient is placed in a supine position and the probe placed near the inguinal ligament (Anesthesia, 2013).

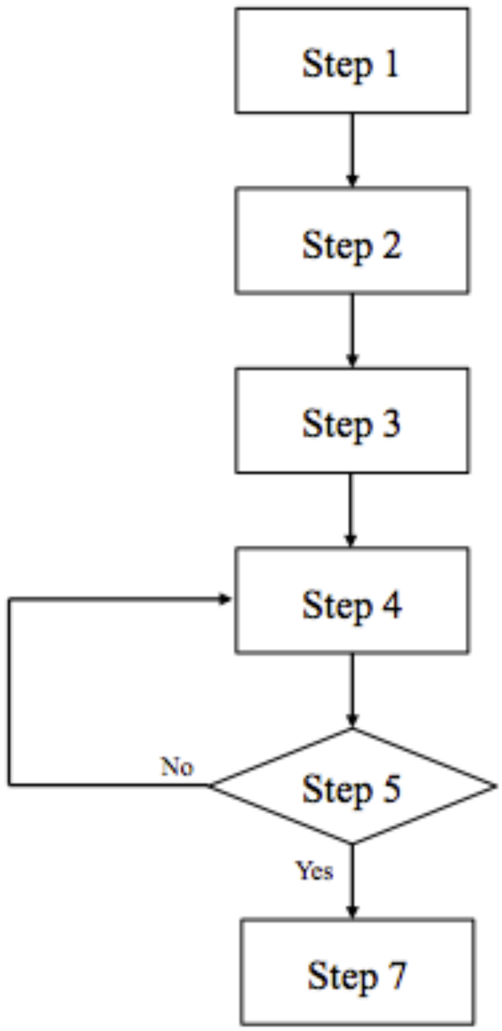

Fig. 9: Flowchart for femoral nerve detection

The femoral nerve differs from the sciatic nerve at the popliteal fossa in that there is only one standard approach for ultrasound-guided nerve block. An anesthesiologist adapted the protocol provided for the nerve block from the guidelines set forth in the literature. The flowchart for the operation given by the NerveGPS software can be seen in Fig. 9 and a detailed description of the steps and the accompanying support instructions are collected in Fig. 10. Steps 1 and 2 guide the user through the setup of the ultrasound platform and the ultrasound transducer placement. Step 3 guides the user through the movement of the probe and the identification of vessels using Doppler. In step 4 the user activates the automated nerve detection. In step 5, if there is agreement between the detection and the anesthesiologist, the clinician should insert the needle (step 6), otherwise they should move the probe as recommended in step 6 before returning to step 5.

	Instructions	Prompt	Picture Display
Step 1	Probe: Linear array transducer Frequency: 8-12 MHz Depth: - 4cm standard patient - 6cm obese patient	Action: Press `'Enter'`	Probe
Step 2	Place transducer perpendicular to the skin in a transverse orientation 2 cm below the inguinal ligament. Turn on and use color Doppler to identify the femoral artery	Action: Press `'Locate Artery'` or `'Enter'`	Probe
Step 3	Once located, put it in the middle of the screen. Turn off color Doppler.	Action: Press `'Capture Nerve'` or `'Enter'`	Inguinal crease and fade into probe and end with sonoanatomy
Step 4	Keep probe still until progress bar is full. Red Circle: Most probable nerve location. Heat map: History of the hits for the program	Action: Wait for progress bar.	Heat map
Step 5	If location is confirmed, perform nerve block, else move probe cranially or caudally in increments of 1 cm and repeat step 2 each time.	Action: Press `'Confirm'` or `'Continue Detection'`	Heat map
Step 6	Insert Needle	Action: Insert needle	-

Fig. 10: Steps for detection of femoral nerve

3. 2. Graphical User Interface

3. 2. 1. Principles of Graphical User Interfaces (GUI)

Graphical user interfaces are the interface between the user and the software he is using. GUIs simplify the interaction between the human and the computer. Successful GUIs are based on several principles of human centered design (Norman, 2002; Norman & Draper, 1986). These concepts are the following:

- **Affordance** refers to the relationship between a person and the interface. Affordances are features that provide the user with information on how they function.
- **Aesthetics** is the organization and appearance of the interface. Aesthetics are key when designing interfaces that users will be interacting with or monitoring over long periods of time. A well-organized interface, with containers regrouping similar objects and controls, simplifies the use of the software by making the functions visible and clear to the user.
- **Familiarity** is the consistency between the software's interface and the tools and programs the user is accustomed to. Familiarity also refers to the consistency that must exist within an interface when performing an action. Consequently, a well-designed interface would provide a "Close Window" button similar in style and location to the one used by the host operating system, or another popular operating system.
- **Mapping** refers to the relationship between the controls offered by the interface and their effects on the program. An essential pillar to design, this concept ensures the intuitiveness of a control. According

to this concept, a checkbox with the label "Show circle" should show the circle when the checkbox is checked and hide it when it isn't.

- Feedback is the information that the user receives from the program after an event to notify him of its completion or progress, or to prompt the user to perform the next event. Feedback can be provided in a variety of forms including visual, audio and tactile.
- Constraints restrict the types of interactions that the user can have with the interface. They manifest themselves through different ways including disabling and/or controls (e.g. buttons, lists) from the user or providing the user with a list of inputs to choose from in a dropdown. This can be done to have the program achieve a certain flow or to prevent the user from providing an undesired input.

(Norman, 2002; Norman & Draper, 1986)

Don Norman states that the application of these design concepts increase the usability of an object. The successful use of these concepts minimizes the gulf of execution and the gulf of evaluation. The gulf of execution refers to the difference between what a user thinks needs to be done to perform a certain action and that which actually needs to be done. The gulf of evaluation refers to the difference between the state or output of a system and the user's ability to assess it.

The pursuit of a well-designed and intuitive interface becomes even more relevant when designing interfaces in medicine and anaesthesia. Anaesthesiologists are presented with a substantial amount of information in the operating room and organizing them to make them easily visible and readily available presents a significant challenge. In addition to the visual displays from patient monitoring, the clinicians can be confronted with external stimuli from alarms, sound, stress of the operation and fatigue (Abolmaesumi, Salcudean, Zhu, Sirouspour, & DiMaio, 2002). A well-designed interface is essential to helping anaesthesiologists perform the correct decisions. The goal of the interface is to highlight the information important to the clinician and prevent adverse events. There are two important displays in anaesthesia: that of the anaesthesia machine and that of the ultrasound platform when performing operations that require ultrasound guidance. The interpretability of each display is important to the success of the operation.

3. 2. 2. Presenting the graphical user interface

The NerveGPS system is launched from an executable on the desktop of the computer. When launching the program, the user is prompted to choose the nerve block they would like to perform (Popliteal or Femoral) and the side (Right or Left) of the patient they would like to perform it on. The user can then press on OK to continue in the program flow. The next panel provides the user with a real-time video panel to the left and instructions to the right.

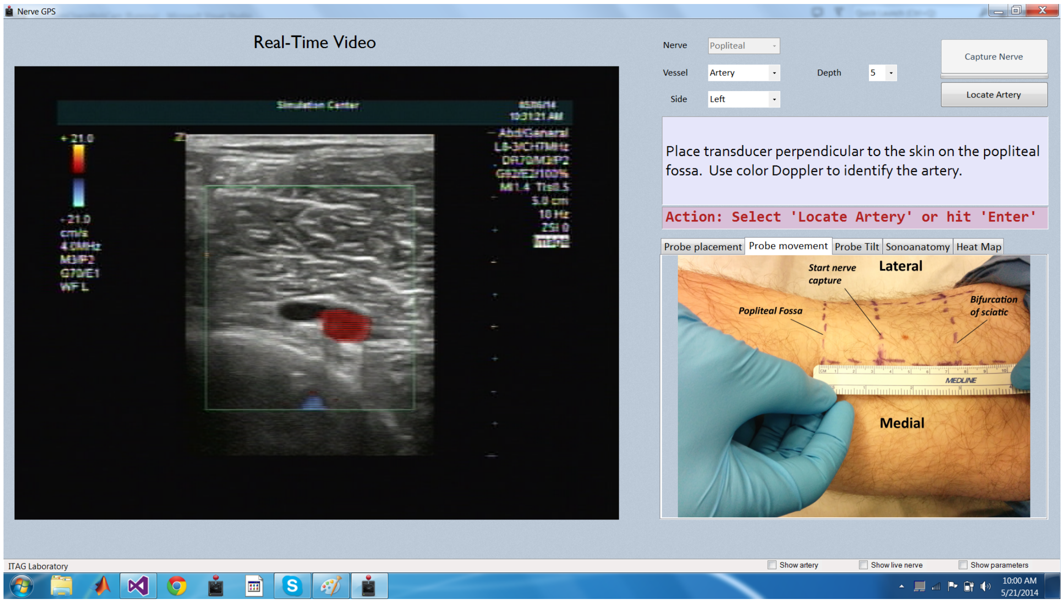

Fig. 11: NerveGPS UI panel with instructions for Step 2

The GUI of the NerveGPS is divided into 3 distinct parts: the real-time video feed that presents the image acquired directly from the ultrasound feed, a section corresponding to instructions for the educational aspect of the program and a section for the main controls used to control the program settings. Figure 11 shows a UI panel of the start of step 5, which is representative of the NerveGPS decision support system. The real time video feed is a direct feed from the ultrasound machine, with the exception of an overlay to indicate the location of the nerve or artery when the functions are enabled. The instructions are broken down into 3 different components:

1. The purple textbox (Figure 12, item 9) provides textual instructions on what current clinical step needs to be taken.
2. The red action text box (Figure 12, item 10) provides the user with the next step that the user needs to perform software-wise after completion of the clinical instructions in the purple text box.
3. The image frame (Figure 12, item 12) presents a visual representation of the software's instructions.

The user can skip forward or backwards between the different steps of the process instructions using the tabs above the image frame (Figure 12, item 11). At the top right of the panel, the user can find buttons and drop down lists to be used in the program. The dropdown lists (Figure 12, item 2, 3, 4, 5) provide the users with the list of allowed inputs of the program for the "Nerve", "Artery", "Side" and "Depth" arguments. When the user changes the depth on the ultrasound platform, they must change the depth in the program using the UI dropdown. The "Capture Nerve" and "Locate Artery" buttons (Figure 12, item 6 & 8) allow the user to activate artery or nerve detection. When the "Capture Nerve" program is launched, it enables the progress bar (Figure 12, item 7).

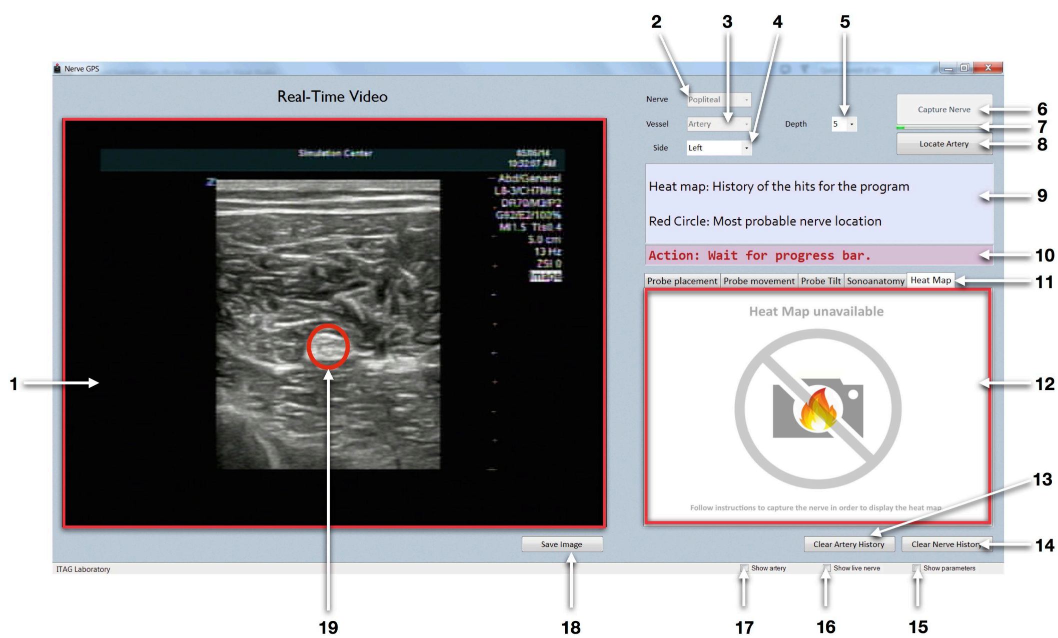

Fig. 12: Presentation of the NerveGPS UI panel

Legend:

1. Live ultrasound video feed *image frame*
2. Nerve selection *dropdown box*
3. Vessel selection *dropdown box*
4. Side selection *dropdown box*

5. Depth selection *dropdown box*
6. Begin nerve capture on live video feed *button*
7. Nerve detection *progress bar*
8. Begin artery location detection *button*
9. *Text box* containing current instructions on how to perform procedure
10. *Text box* indicating the next action to take by the clinician
11. *Tabs* to navigate to jump to past or future instructions
12. *Image frame* containing instructions on how to perform procedure
13. *Button* to clear the stored location of the artery
14. *Button* to clear the history of located nerves
15. *Checkbox* to toggle the display of parameters to monitor algorithm debugging parameters
16. *Checkbox* to toggle displaying the location of the last nerve detection
17. *Checkbox* to toggle displaying the location of the artery
18. *Button* to save currently displayed ultrasound image for later analysis
19. Red circle indicating the most probable location of the nerve based on the history of nerve detections

The suggested nerve location marked by a red circle (Figure 12, item 19) is determined using the data collected from running the nerve detection software for 20 seconds. A red circle represents the nerve for ease of use to mimic the circularity of the needle. The result of each nerve detection is compiled into the heat map as seen in Figure 13, which is displayed in the UI in the instruction image box (Figure 12, item 12) and accessible via the above tab marked "Heat Map" (Figure 12, item 11). The heat map displays the areas with the most hits in warmer colors (red) and those with the least in colder colors (blue).

At the bottom of the GUI are the "Clear Artery History" (Figure 12, item 14) and "Clear Nerve History" (Figure 12, item 13) buttons, which can be used to interrupt the nerve and artery detection programs and clear the location of the nerve or the artery from the program. The GUI also gives the user the option to save the image currently being shown on the live feed. The ribbon at the bottom features three checkboxes that enable developer-troubleshooting information. The “Show artery” checkbox (Figure 12, item 17) shows the stored location of the artery as a green circle. The “Show live nerve” checkbox (Figure 12, item 16) shows the location of the most recent result of the automated nerve detection. The “Show parameters” checkbox shows 5 input text boxes in which to modify the weights of the regional descriptor arguments being passed into the function and an output textbox to show noteworthy console output.

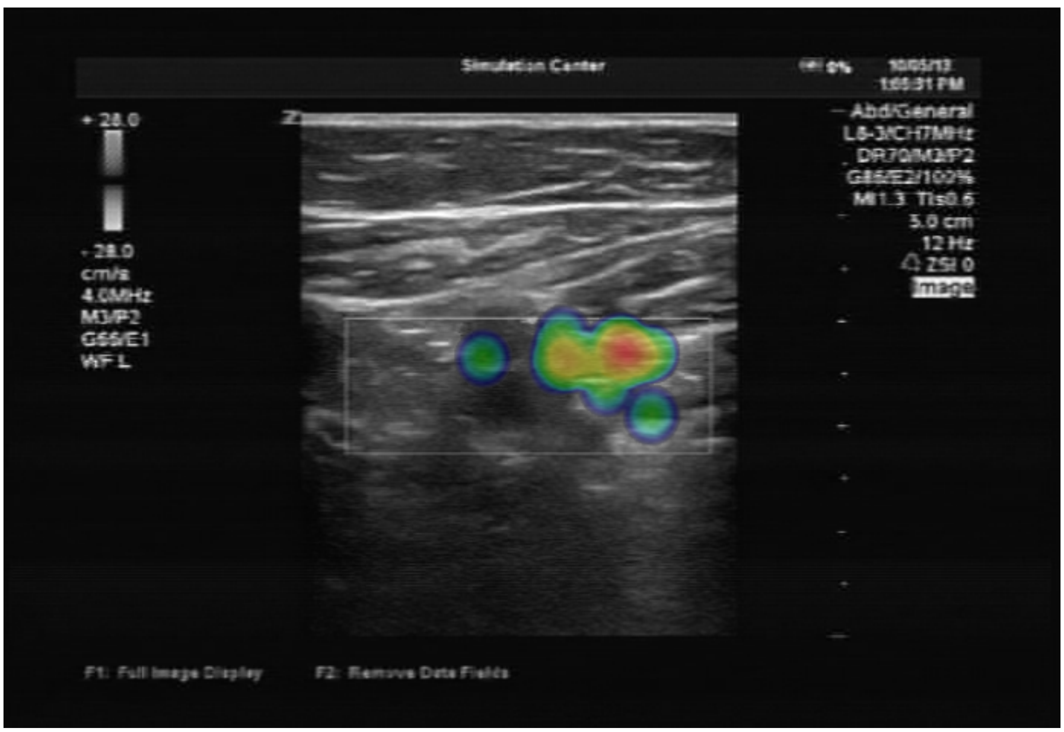

Fig. 13: Example heat map for femoral nerve detection

To guide the user through the flow of the procedure, the program restricts the use of some features such as the artery detection or nerve detection buttons by disabling the buttons that call them. As a result, the program is restricting erroneous inputs and facilitating the task of the user by making the important controls more prominent and visible

3. 3. User feedback

The interface went through several versions using feedback from the users. Users included a trained anaesthesiologist, two anaesthesia research fellows and two engineers. During each test the users would attempt to locate the nerve following the NerveGPS protocol. After these trials, the user interface was modified to incorporate feedback.

• Chapter 4 – Nerve detection algorithm

4. 1. Overview

The automated nerve detection algorithm for ultrasound nerve block guidance is included as part of the NerveGPS decision support system. Given the placement of the probe in the desired region of interest, the clinician can activate the nerve detection software to obtain a suggestion of the nerve location. As mentioned in previous sections, difference in anatomies in nerve block regions make it essential to have distinct versions of the software for each region. The following section will detail the algorithm used to detect the sciatic nerve at the popliteal fossa and then present the changes made to adapt it for the femoral anatomy.

The nerve detection algorithm consists of 6 image processing steps. Once the input has been captured, the appropriate algorithm is executed on the input. The algorithm first uses a filter to reduce the amount of speckle noise in the ultrasound image and histogram matching to normalize the image contrast. The image is segmented for easier analysis and dimension analysis is performed on the resulting objects for feature extraction. The objects are then scored to determine the most nerve-like object. The results of the scoring algorithm are then verified using active contours to determine the final location of the nerve if it is present within the ultrasound image.

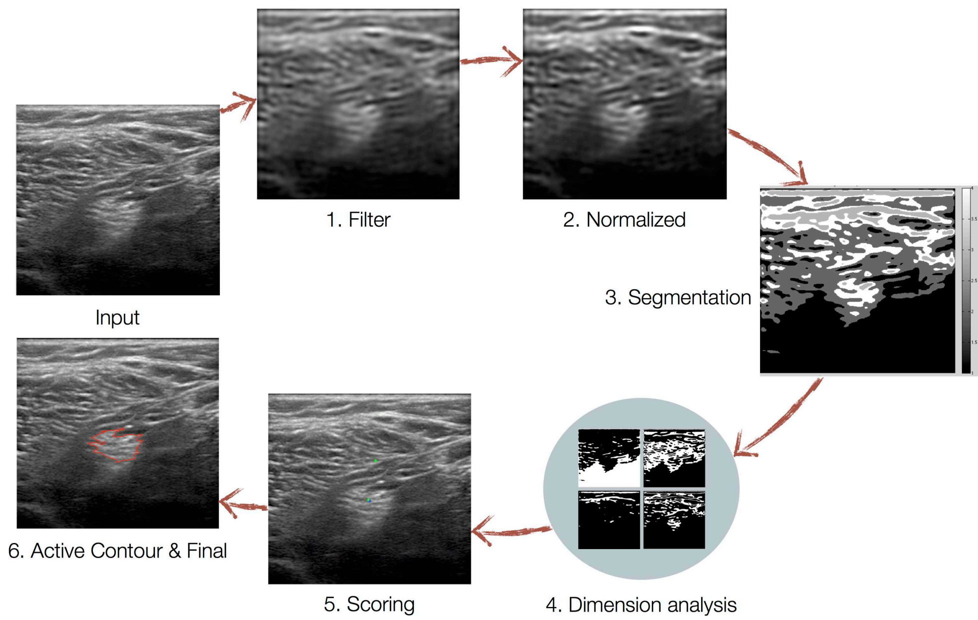

Fig. 14: Overview of the sciatic nerve detection image-processing flowchart

4. 2. Image acquisition

All tests were performed using a Zonare (Mountain View, CA, USA) z.one ultrasound platform. The live ultrasound feed was acquired using the ultrasound platform's HDMI output (1280x1024). The Audio Video Equipment Device (AVED) by Zonare then converts the image to video composite format (720 x 480). The image is fed in composite format into a Dazzle DVD recorder frame grabber developed by Pinnacle Systems (Mountain View, CA, USA). The frame grabber is connected to an ASUS (Taipei, Taiwan) Zenbook Prime UX31A computer (1.7GHz Core i5-3317U) via USB. The image is then integrated into the GUI using a .NET framework for C# that enables access to Microsoft's DirectShow Application Programming Interface (API) for media streaming and video capture in Windows. Image processing is performed on individual frames. The software analyzes one frame at a time while the live video feed plays, capturing the current frame as a new frame from the live stream after the end of the algorithm execution on the previous frame. A flowchart illustrating the image acquisition process is provided in Fig. 15.

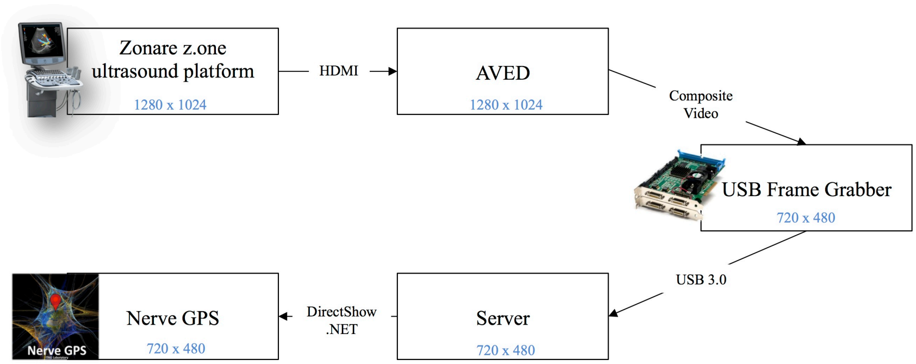

Fig. 15: Image acquisition flowchart

4. 3. Filter

4. 3. 1. Speckle noise filtering

Ultrasound speckle noise is a random interference pattern formed with coherent radiation of a medium containing many sub-resolution scatterers (Anderson & Trahey, 2000). The nature of speckle pattern depends mainly on the number of scatterers per resolution cell or Scatterer Number Density (SND). As seen in section 2.3.2 ('Ultrasound image filtering'), the reduction of speckle noise is the key to obtaining a better ultrasound image. The following section details the methodology used to find the filter in the NerveGPS automated nerve detection algorithm.

4. 3. 2. Black box testing

As outlined in section 2.3.2 ('Ultrasound image filtering'), there are a multitude of different filters that exist for eliminating or reducing noise in an image. Wavelet decomposition filters are commonly used for the reduction of speckle noise in ultrasound diagnostic imaging to reduce the loss of detail during filtering. In the literature, research for diagnostic purposes often employs wavelet filtering to avoid the loss of small details that may be crucial to the diagnostic. Despite this predilection for wavelet filters in most ultrasound image processing research, an array of different filters was evaluated to determine the best fit for the NerveGPS. To assess the fit, a black box testing methodology was used. 5 ultrasound images from the sciatic and femoral areas from different participants were run through the filters outlined below. The filters were chosen to represent the filters most often used to reduce ultrasound speckle noise (Loizou et al., 2005). To evaluate the fit, the resulting filtered images were inspected visually to identify whether the filter had made the principal anatomical elements in the image more defined. The resulting images that provided the best visual fit were then segmented to see which filter provided the best image for segmentation.

To perform the black box testing, the following filters were used:

- No filter
- Wiener filter (Taxt & Strand, 2001)
- Ideal filter
- Butterworth filter (Mateo & Fernández-Caballero, 2009)

- Wavelet filter (Gupta, Chauhan, & Sexana, 2004; Yue, Croitoru, Bidani, Zwischenberger, & Clark, 2006)
- Median filter (Czerwinski, Jones, & O'Brien, 1995)
- Homomorphic Ideal filter (Taxt, 1995)
- Homomorphic Butterworth filter
- Homomorphic Wavelet filter

The wavelet filter was included as one of the most probable choices for the black box testing. Wavelet filters were tested using different wavelet types and decomposition levels with bands eliminated LH, HL, HH and LH-HH using the MATLAB 2013a wavelet toolbox (Figure 16). The NerveGPS software only requires the identification of larger elements within the image, the Wiener filter was found to be suited for this application. The Wiener filter is designed to remove Gaussian noise from an image. The Wiener filter is rarely chosen for diagnostic applications because the ultrasound speckle noise does not have a Gaussian distribution, which leads to loss of detail when the Wiener filter is applied. The Butterworth filter is a spectrally steep low pass filter. It provides the software with a filtered image that is blurred but removes much of the noise and detail around the largest anatomical elements, for an easier visualization of these elements. The median and ideal filters were included but did not provide a good match. To determine the necessity of the filter (removing the filter would represent a decrease in the software runtime), the software was also tested without a filter. The software was tested using a combination of filters. Two of more filters resulted in an increase in software runtime and little improvement in image quality. After testing, the Butterworth filter was identified as the filter that would give the best results and was thus the most adapted for this application.

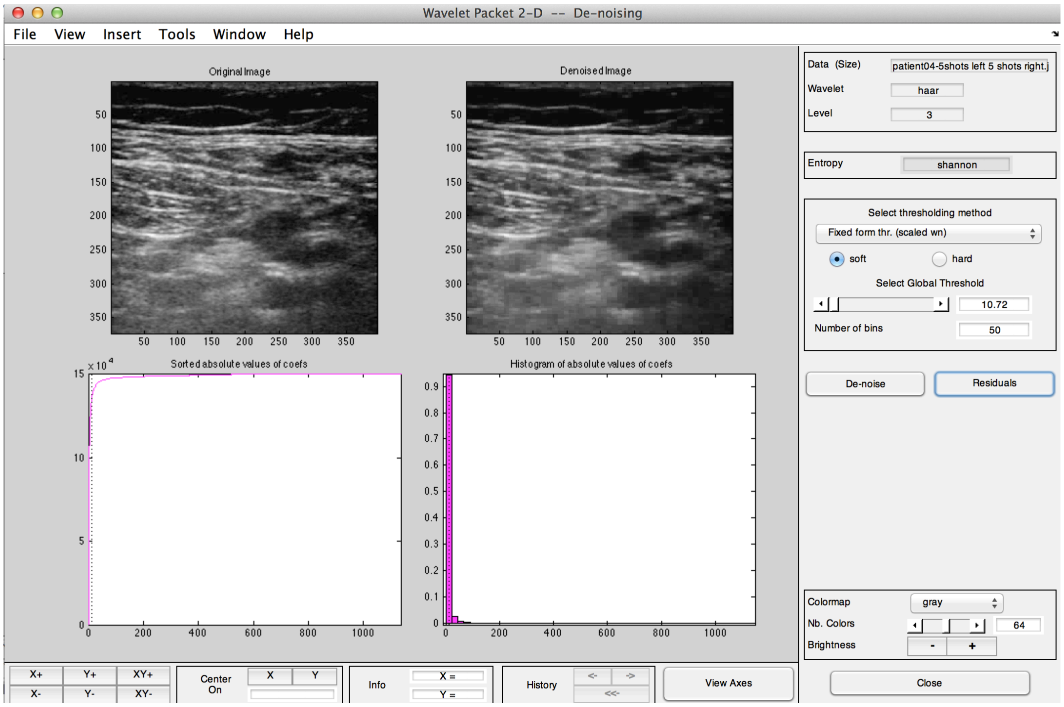

Fig. 16: MATLAB's wavelet toolbox being used for an ultrasound image

4. 4. Histogram matching

When performing ultrasound guided nerve blocks, the anaesthesiologist can change the contrast settings on the ultrasound platform to better visualize the nerve. The differences in pixel intensity make standardization necessary. To facilitate the analysis of the images the software normalizes the contrast for each image using histogram matching. Histogram matching is the adaptation of the frequency distribution of an image's pixel intensities to that of a representative reference image. For each region of interest, sample images were selected that were representative of the sonoanatomy. After filtering, the filtered image's histogram was compared to the reference histogram to normalize contrast. The histogram normalization process is illustrated in Figure 17. The initial image a) appears bright with a peak in the histogram for a grayscale pixel intensity of approximately 60, as seen in c). After histogram matching in b), the image intensity resembles that of the reference image, with the non-echoic structures such as the vessels appearing darker. The change can be seen clearly in the histogram of the resulting images in d) which shows frequency peaks at around 10 to 20 pixels.

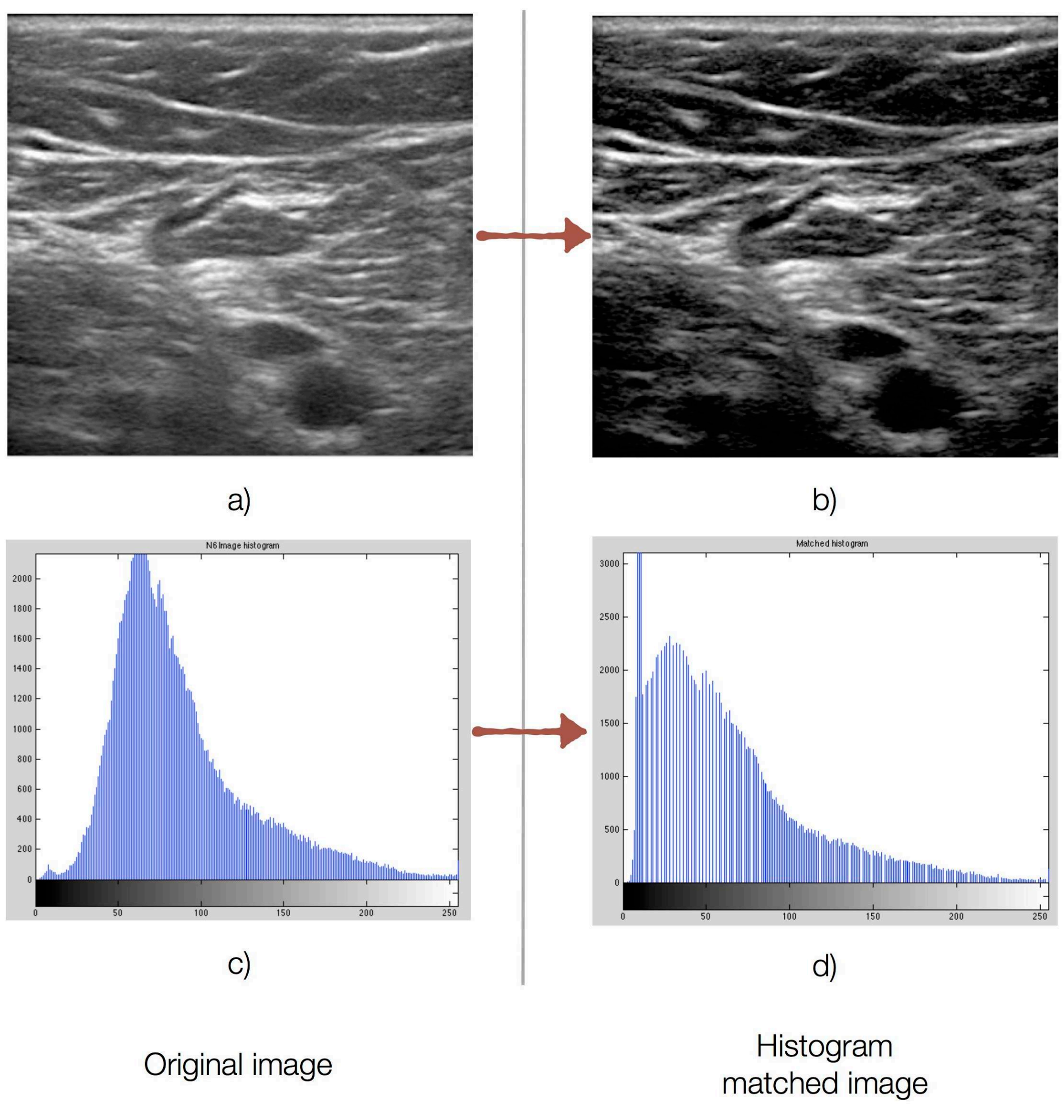

Fig. 17: Histogram matching results on an image of the popliteal nerve. Figures a) & c) are the original image and its intensity histogram respectively and figures b) & d) are the resulting image and its histogram respectively.

4. 4. Image segmentation

Image segmentation allows for the simplification of image processing by segmenting an image into a smaller number of groups. Several options exist, however the method most suited for this application was k-means. This section will describe the k-means segmentation process used.

4. 4. 1. K-means

K-means is an iterative clustering algorithm for grouping points into n clusters. To perform the clustering, n points are randomly selected and the rest of the points are grouped around these points based on their similarity with the specified characteristics using a squared Euclidean approach. Once the clusters are formed, the point nearest to the mean of each cluster is used to group the pixels into n clusters again. The previous operation is repeated until the point nearest to the average is the same point as that of the previous iteration. For the NerveGPS algorithm, the points are grouped into 4 clusters for k-means clustering based on intensity. Grouping the points into 4 clusters allows for the identification of larger objects which otherwise would not have been possible. The number of clusters used was determined heuristically. Empty clusters are handled by creating a new cluster consisting of the one point that is the furthest from its mean. The results of k-means clustering segmentation is illustrated in Figure 18. Figure 18 a) shows the original image and b) shows the result of k-means clustering image segmentation into 4 clusters. The 4 images in the blue oval at the bottom of Figure 18 represent the binary image of each cluster.

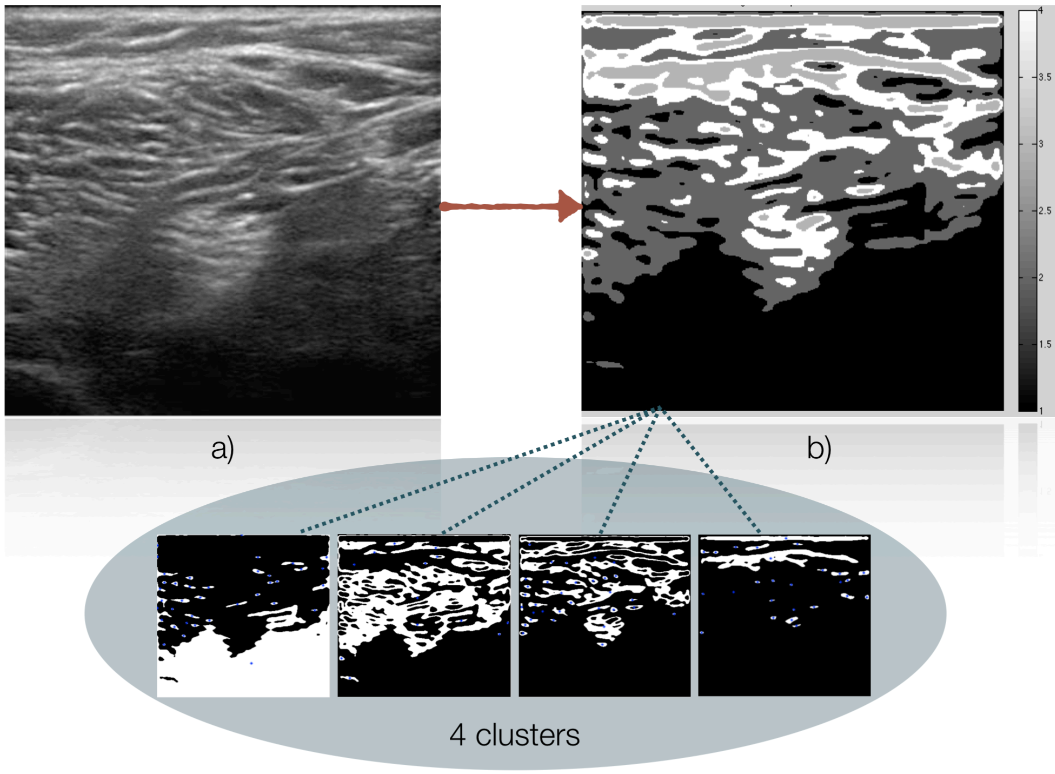

Fig. 18: a) and b) represent the images before and after k-means respectively. At bottom, binary images representing each intensity cluster. Illustration of results of k-means for image segmentation of sciatic nerve ultrasound image.

4. 5. Scoring

After segmentation of the image, feature extraction determines the objects in the image that most likely to correspond to the location of the nerve. An object is defined as a contiguous region of points with value '1' within the binary image using 4-way connectivity. The defining anatomical properties of a nerve are its hyperechoicity and oval shape, which distinguish it from the surrounding elements. Within the nerve, a honeycomb like structure can be seen in ultrasound, representing the nerve fascicles within their oval shaped sheath. A scoring algorithm based on the regional descriptors of each object was used to perform feature extraction. Each object is assigned a score corresponding to how likely the object is to be the nerve of interest. The following regional properties for each object of interest were pre-processed to compute the score:

i. **Intensity** – Intensity represents the color of the object within the grayscale image. Intensity is computed as the mean intensity over all the points in the object and is contained between 0 and 255, with 0 being black and 255 being white.

ii. **Area** – Area is calculated as the total number of pixels per object using 4-way connectivity.

iii. **Eccentricity/Compactness** (Nixon, 2008) – Compactness is one of the measures used to determine the oval shape of the objects. The eccentricity dimension is contained between 0 and 1. Compactness is a measure of the shape of the object and is defined as the ratio of perimeter to area:

$$Compactness = \frac{4\pi * Area}{Perimeter^2}$$

iv. **Height-to-Width** – The ratio of height to width is used to remove long and thin objects such as muscle fascia. It is also one of the measures used to determine the oval shape of an object. This property is contained between 0 and 1.

v. **Extent** – Extent is the ratio of the number of pixels in the object to the number of pixels in the objects bounding box. This property is contained between 0 and 1.

To decrease the runtime of the algorithm, this analysis is done only on the objects within the three brightest layers. The following sections describe how the dimensions of the analyzed objects are gathered to compute the object's score.

4. 5. 1. Data collection

All 5 regional properties are given a weight based on their importance and uniqueness in distinguishing the nerve from other objects. To determine the weights, the dimensions of every object within a 100-image sample were computed. Within these objects, those that corresponded to the nerve were identified. The dimensions of the nerve and all other objects were aggregated and compared. Figures 19 to 23 illustrate the results of the aggregation and the data used for comparison.

The areas of the nerves (red dots) are similar and contained between 800 and 10 000 pixels per object whereas the other objects are more scattered (Figure 19).

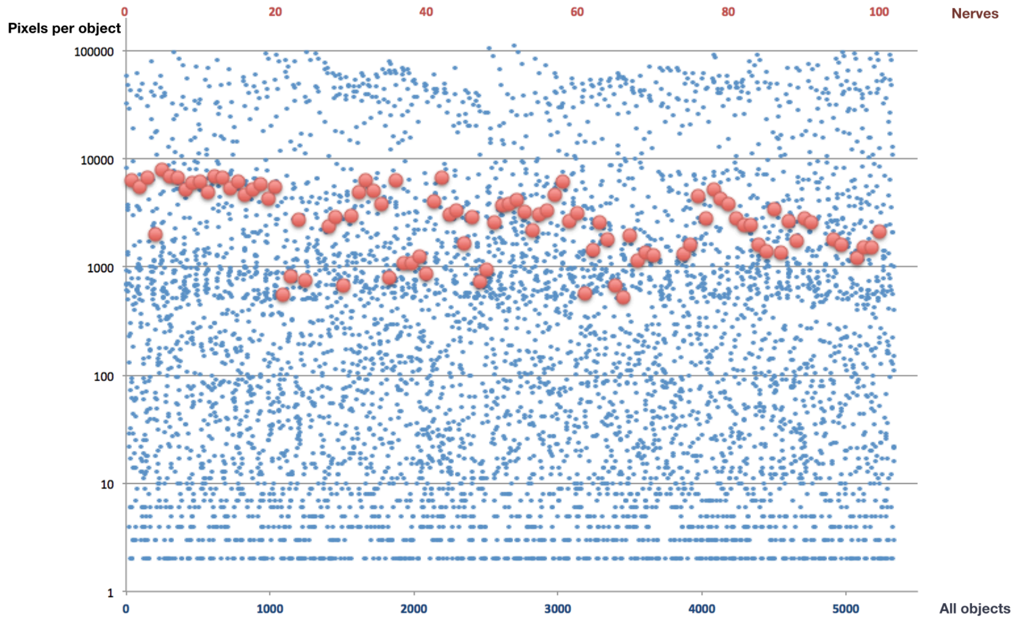

Fig. 19: The area distribution of all objects is represented in blue and those that correspond to nerves in red. The graph presents the distribution of the area regional descriptor for all objects compared to the nerves. The y-axis has a logarithmic scale and represents the number of pixels per object.

The eccentricities of the nerves are grouped between 0.1 and 0.65 with over 50% of the nerves between 0.15 and 0.3. The other objects are scattered between 0 and 1 with peaks for an eccentricity of 1 and a high concentration for eccentricities below 0.2 (Figure 20).

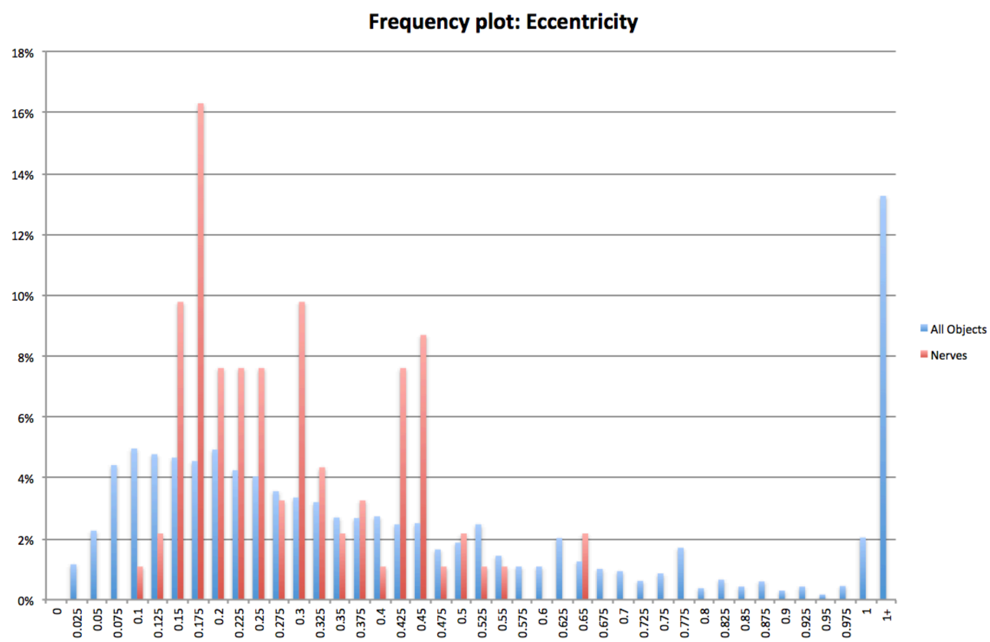

Fig. 20: Graph representing the eccentricity/compactness distribution of all objects (blue) and those that correspond to nerves (red). The graph is a frequency plot representing the eccentricity/compactness regional descriptor of all objects (blue bars) compared to that of the nerves (red bars).

The extent of the nerves is contained between 0.3 and 0.75 and that they have a normal distribution. The extent for the other objects is also normally distributed between 0 and 1 with a peak at 1 (Figure 21).

The intensity of the nerves is contained between 75 and 190 with peaks for intensities around 90, 120 and 150. The other objects have intensities ranging from 0 to 255 with a high concentration for intensities below 100 (Figure 22).

The height-to-width ratio of the nerve is contained between 0.225 and 0.975 with a distribution similar to normal. The other objects have values between 0 and 1 with the majority having a value of 0.5 or below 0.3 (Figure 23).

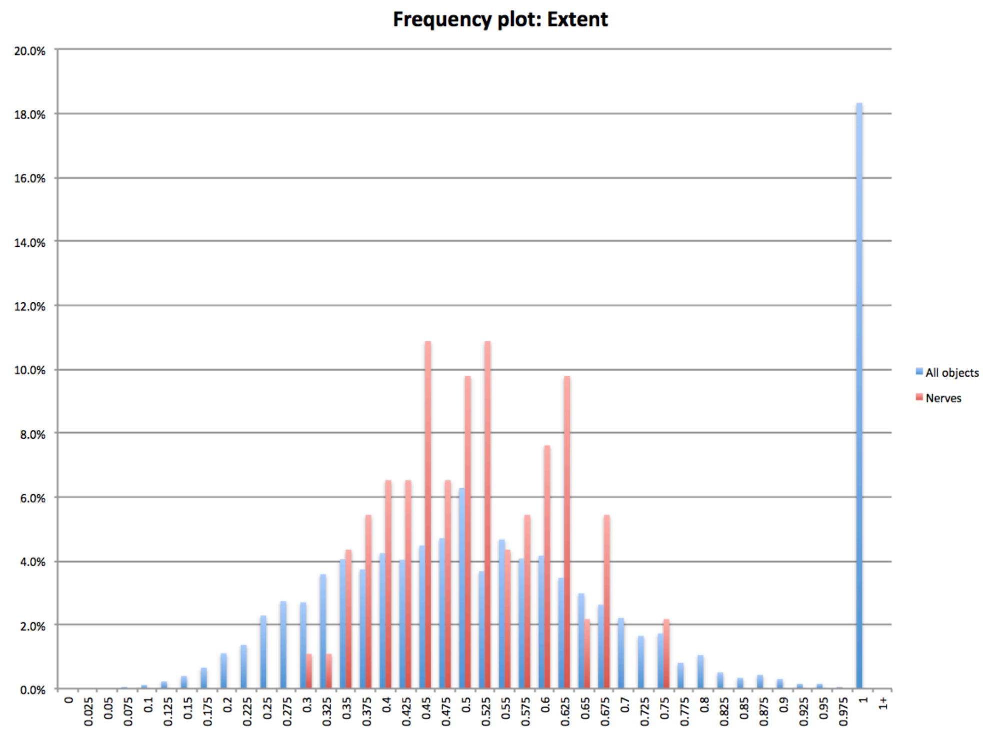

Fig. 21: Frequency plot representing the extent regional descriptor of all objects (blue bars) compared to that of the nerves (red bars).

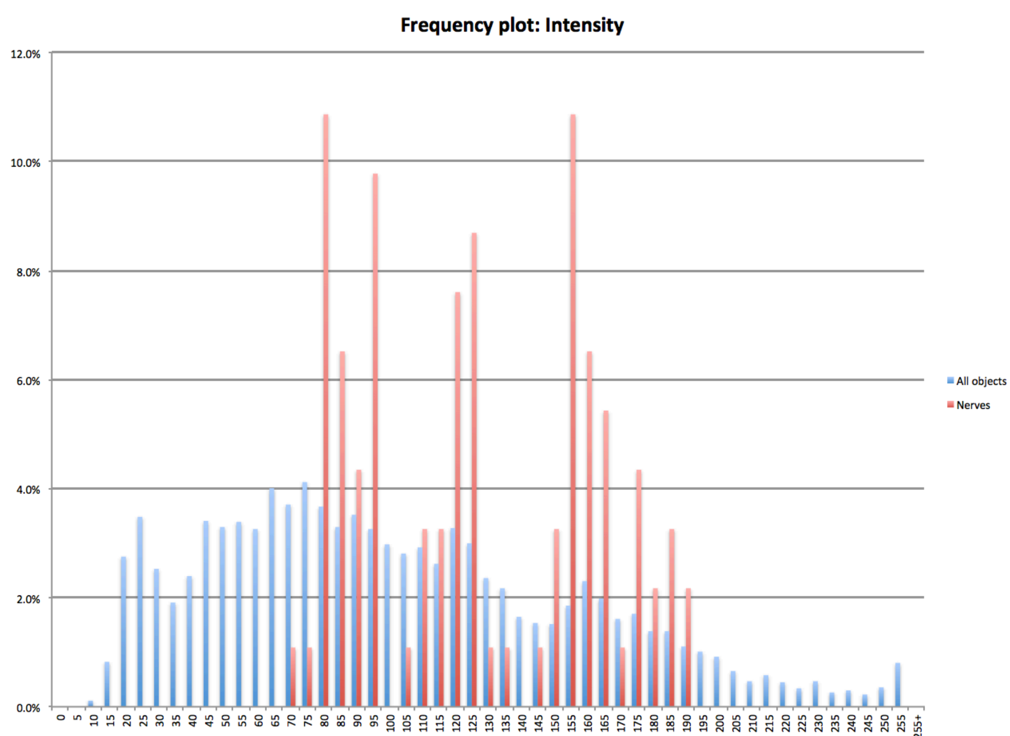

Fig. 22: Frequency plots representing the intensity regional descriptor of all objects (blue bars) compared to that of the nerves (red bars).

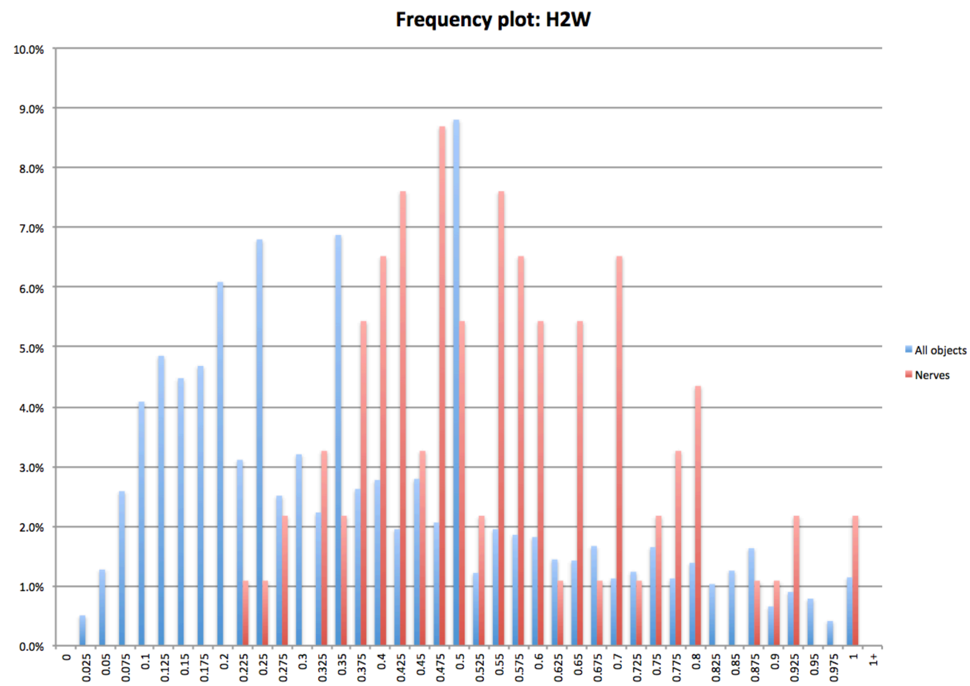

Fig. 23: Frequency plots representing the height-to-width regional descriptor of all objects (blue bars) compared to that of the nerves (red bars).

The nerves are grouped together for each regional descriptor. The data obtained from the regional descriptors is used to score the objects in the image.

4. 5. 2. Determining weights

Weights allow the software to give more importance to a regional descriptor. Using the data outlined above and heuristic methods we were able to determine the weights as shown in Table 1. The intensity regional descriptor is given the highest importance and constitutes 35% of the total score because of the importance of the nerve's hyperechoicity for the detection.

Eccentricity and Height-to-Width, the properties used to evaluate the shape of the object, represent 13% and 17% of the score respectively for a total of 27%. The complete breakdown of weights for the regional descriptors is given in Table 1.

Descriptor	Weight
Intensity	35
Area	25
Eccentricity	13
Height-to-Width	14
Extent	14

Table 1: Weight distribution for each descriptor

The values of the regional descriptors are mapped to low or band pass type curves with different scalars to give each regional descriptor a score using the data on the standard properties of a nerve:

$$Score = -\frac{1}{a}e^{(Value+b)} + c$$

The intensity score can be a maximum of 1. For intensity values above the average the given score decreases slowly at an exponential rate, to reach 0.5 for 255. For below average intensity values, the given score decreases at an exponential rate, reaching 0 at intensity value 75. 75 is the lower boundary for the standard intensity of the nerve (cf. Figure 22). Below the lower boundary the score continues to decreases, returning negative values for scores. The intensity score is then weighted as seen above and added to the total score (Figure 24).

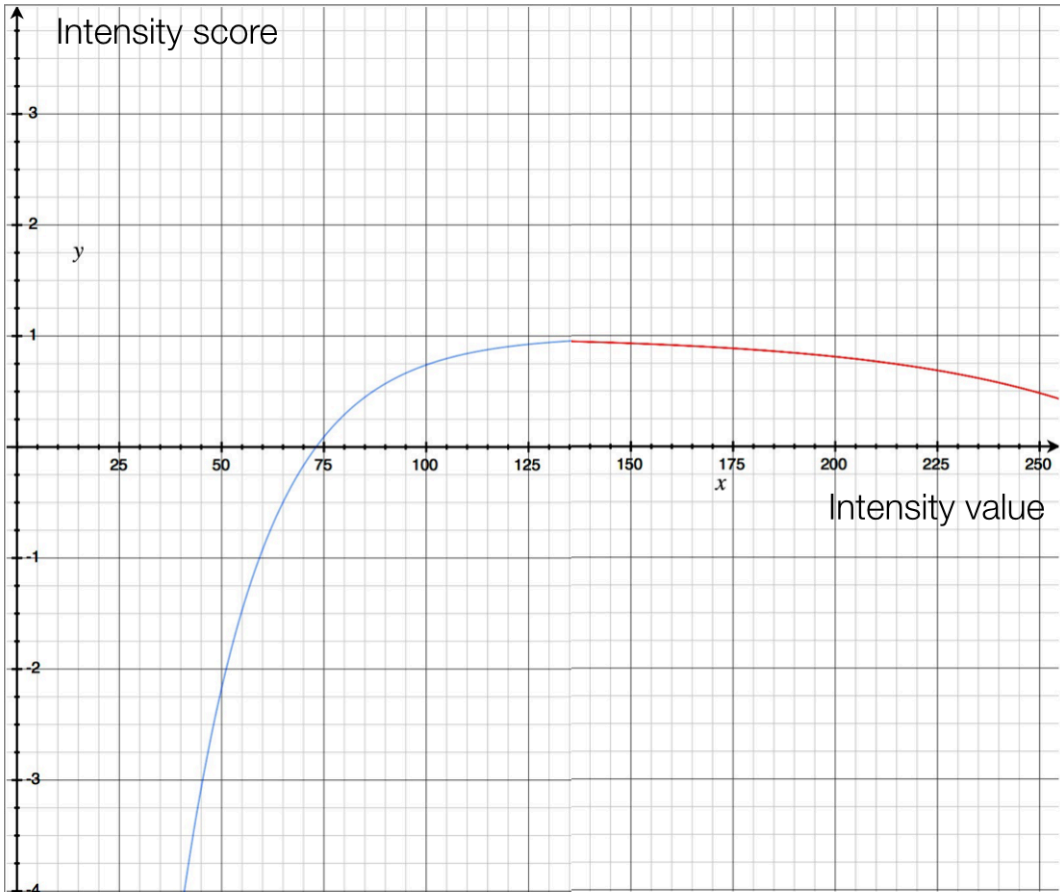

Fig. 24: Graph illustrating the mapping of values to scores for the intensity regional descriptor. The y-axis represents the score before weighting (this score can have a maximum of 1) and the x-axis represents the value of the intensities between 0 and 255.

4. 5. 3. Edge cases and extrema settings

The nerve is superficial to the artery and vein and more profound than the muscle fascia above. These anatomical properties of the nerve can be integrated into the software, minimizing the area on which the algorithm is applied. When possible, these elements are located to set upper and lower boundaries of analysis. Reducing the area of analysis as seen in Figure 25 allows for increased precision and decreased runtime. To locate the vessels, the software makes use of the color Doppler function. The algorithm uses a function to search through the red and blue color spaces of the image. Thresholding is then applied to obtain a binary image containing only the surface area of the vessel. Objects from the binary image with area contained in a defined interval are identified as the vessel. The y-coordinate of the topmost pixel of the object is chosen as the lower limit for boundary for image cropping. To locate the muscle fascia, regional descriptors are used to find an object with dimensions similar to the muscle fascia. The muscle fascia appears in ultrasound as a long thin strand at the top of the image. If the program finds an object with a very low high to width ratio and is more than 70% of the image in width, then its centroid is used as the upper limit for cropping.

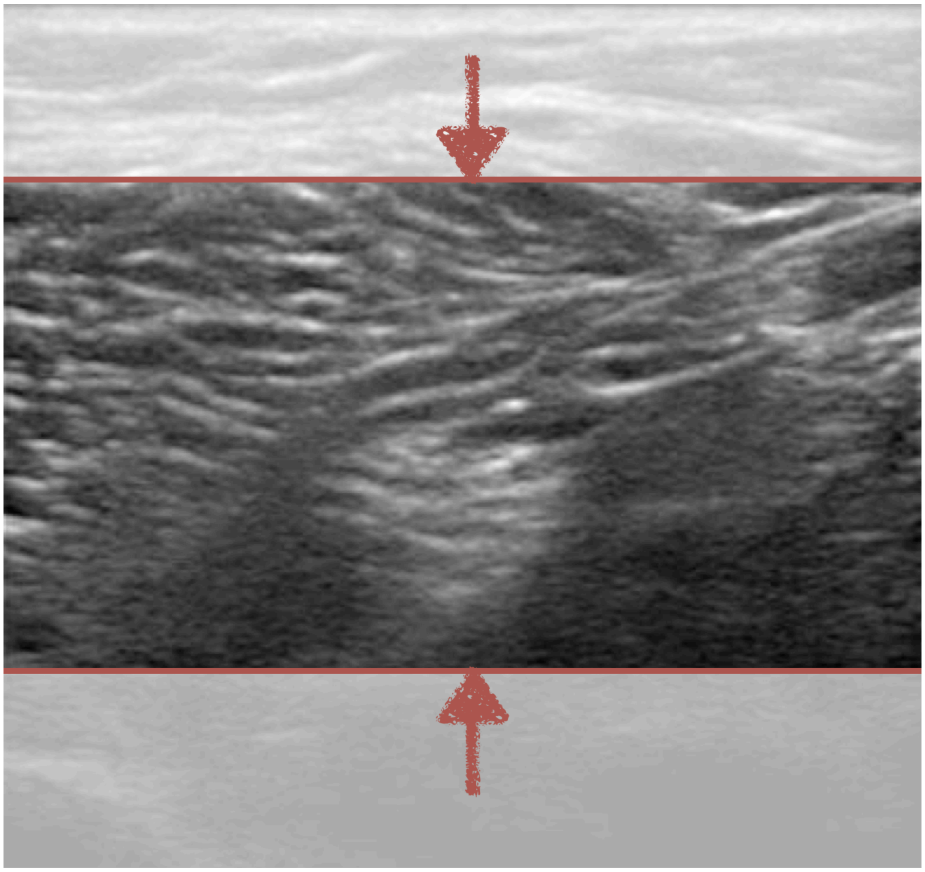

Fig. 25: Region boundaries set by anatomical landmarks on an ultrasound image in the sciatic region: skin & fascia at top and vessels at bottom.

4. 6. Active Contours

Chan Vese active contour modeling is used. Chan Vese active contour modelling can detect objects without defined gradients (Tony F. Chan, 2001). Active contour modeling is used on the bounding box of the object determined to be the nerve. The algorithm grows the contour to match the container object for a more detailed contour of the nerve. The regional descriptors of the contours are then analyzed. Moreover, it provides increased accuracy of the program. Figure 26 illustrates the method and sample results on an ultrasound image of the sciatic nerve.

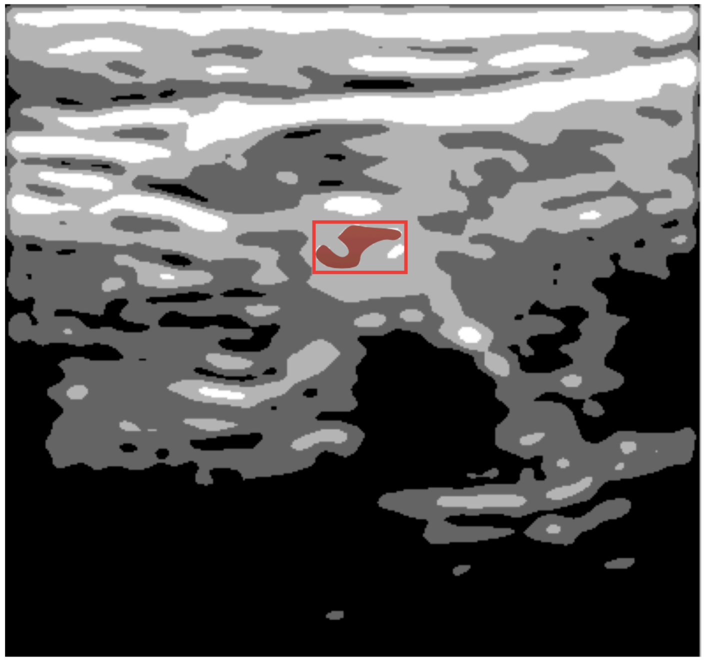

a)

b)

Fig. 26: Illustration of active contours. Figure a) shows the k-means segmented image with the object determined as the nerve shaded in red and the red bounding box used to grow the contour. Figure b) shows the result of the active contour growing

4. 7. Final Score

The voting algorithm provides the 3 objects that are the most likely to be the nerve according to their regional descriptors. These top 3 objects are sorted in order of decreasing score. The bounding box of the highest scored object is then expanded using active contours and the boundary of the resulting object is scored using the same scoring algorithm. If the score of the latter boundary is superior to a determined threshold score (~75) then the object is determined to be the nerve.

Figure 27 and table 2 illustrate the final scoring process. In Figure 27 b) we can see the center of the 3 objects provided by the voting algorithm. The red star marked as 1 corresponds to the most likely object with the highest score (89) as can be seen in Table 2. The scores for each parameter of this object are also provided in Table 2. Figure 27 a) shows the output of the k-means algorithm to illustrate the objects that the stars correspond to in Figure 27 b). For this image, active contours yielded a score of 86 for the object marked as 1. Since the score was above the score threshold, the object was determined to be the nerve.

The program outputs the final score to calculate the confidence interval and the coordinates of the object that corresponds to the nerve.

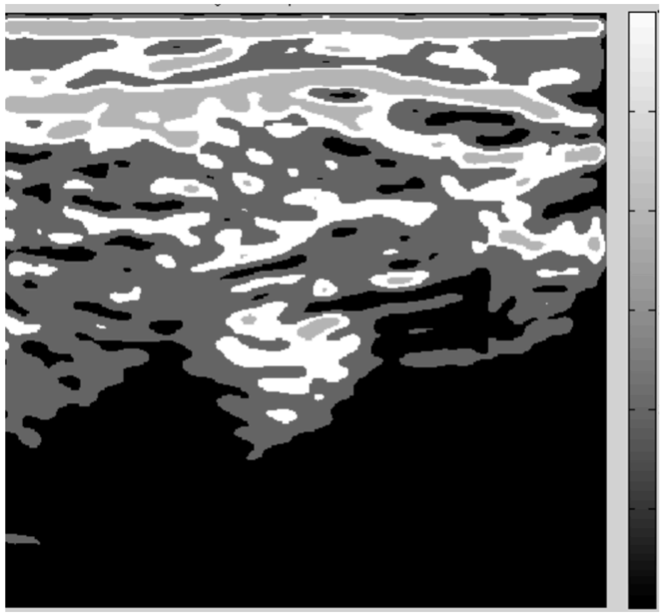

a)

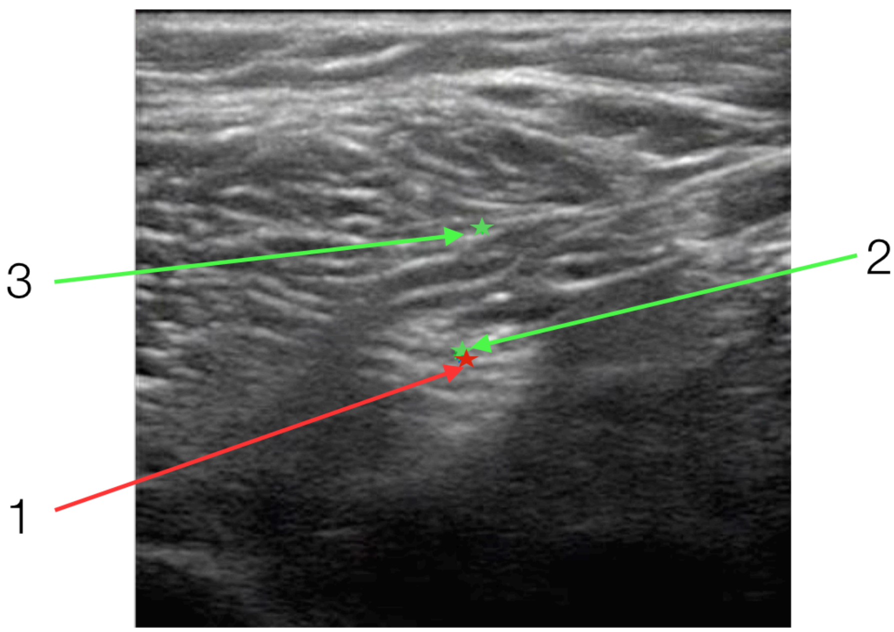

b)

Fig. 27: Ultrasound image of the sciatic nerve, annotated to show location of objects most likely to be the nerve. Figure a) shows the image segmentation output and Figure b) shows the centroids of the objects most likely to be the nerve. (cf. Table 2). Figure a) shows the output of the k-means algorithm to

illustrate the objects that the stars correspond to in Figure b). In Figure b) we can see the center of the 3 objects provided by the voting algorithm. The red star marked as 1 corresponds to the most likely object with the highest score (89) as can be seen in Table 2.

	Score	Coordinates	Intensity	Area	Eccentricity	H2W ratio	Extent
1	89	(197, 210)	116	3384	0.251	0.688	0.568
2	82	(195, 208)	121	1920	0.287	0.631	0.431
3	76	(209, 132)	111	2761	0.126	0.362	0.298
Contour	86	(197, 210)	113	4296	0.175	0.627	0.524

Table 2: Breakdown of scores with individual weights for the objects seen in Figure 27

• Chapter 5 – Testing & Results

To test the systems, the algorithm and decision support system aspects of the project were tested. This section presents the methods used and the results.

5. 1. Study setup

The algorithm and decision support aspects of the system were tested using the same setup. To test the algorithm, the study area was setup in the usual way in which ultrasound guided nerve blockade is usually performed. The patient was positioned on a stretcher in the desired position for the procedure with an ultrasound machine beside the stretcher. The ultrasound machine was connected to a computer via a frame grabber and the images and videos were recorded and stored using Pinnacle Studio 14 (Pinnacle Systems, Mountain View, CA, USA).

To test the decision support system, the study was setup to emulate the conditions when performing an ultrasound guided nerve block. This setup was used test the adequacy of the system as a training or decision support system tool. The setup used is shown in Figure 28. The patient was positioned on a stretcher with an ultrasound machine at arms reach. The ultrasound machine was connected to the computer running the NerveGPS software via a USB frame grabber. The display of the computer running the NerveGPS was mirrored onto a large television to allow the anaesthesiologist to easily follow the instructions given by the program and the results of the nerve detection algorithm. Finally, to capture the feed without consuming CPU cycles a camcorder was used in some trials to film the NerveGPS feed for later review of the performance of the software.

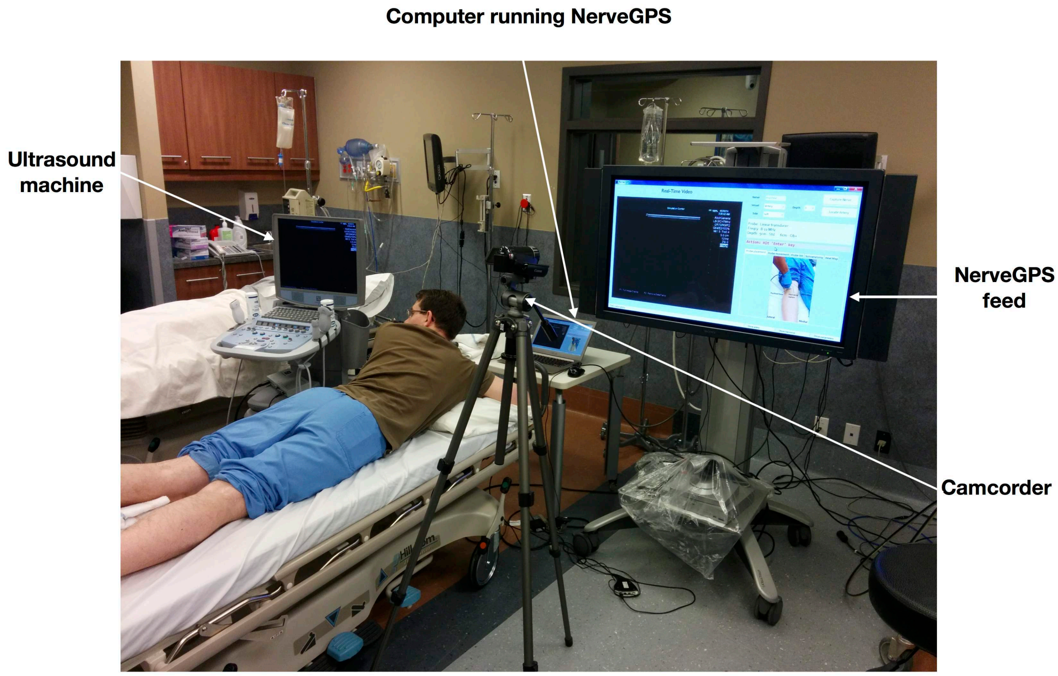

Fig. 28: Setup for the study

5. 1. 1. Study Design

The study was divided into 3 parts:

I. Image analysis – Ultrasound images of the regions of interest were collected from participants and fed into the system for analysis. Image analysis was used to assess the accuracy of the software. Image analysis focused on determining whether the center of the region determined to be the nerve was contained within the region determined by an anaesthesiologist to be a nerve. It is also used to check the overlap between the 2 regions.

II. Video analysis – Ultrasound videos of the regions of interested were collected from participants and then analyzed by the system. Video analysis was used to test if the software's runtime would allow it to be used for real-time video analysis and also test the accuracy of the software (whether or not the nerve was detected).

III. Decision Support System testing – An anaesthesiologist attempted to perform the nerve block following the procedure and guidance provided by the decision support system. The goal of this part was to validate the ability to use the system as a training tool or to provide a second opinion.

This analysis was repeated for each nerve of interest.

5. 1. 1. 1. Protocol

This section will first go over the protocol used for the popliteal nerve and the protocol used for the femoral.

For the popliteal nerve, in part I of the study, 5 participants are imaged bilaterally. Using the trace back approach, 10 images are obtained from each side of the participants for a total of 100 images. Images are obtained in 0.5 cm increments from the popliteal fossa up to the division of the sciatic nerve, as show in Figure 29. Images are only captured if the nerve can be seen in the ultrasound feed. In part II of the study, for the video analysis component, 6 participants are imaged bilaterally in the same way as in part I using the trace back approach, pausing for 5 to 10 seconds every 0.5 cm when the nerve can be seen in the ultrasound feed. Video of the ultrasound feed is recorded from the popliteal fossa to 1 cm above the bifurcation of the sciatic nerve. For part III of the study, the decision support component, the NerveGPS is tested on 2 participants. The anaesthesiologist is asked to open the software and follow the instructions given exactly.

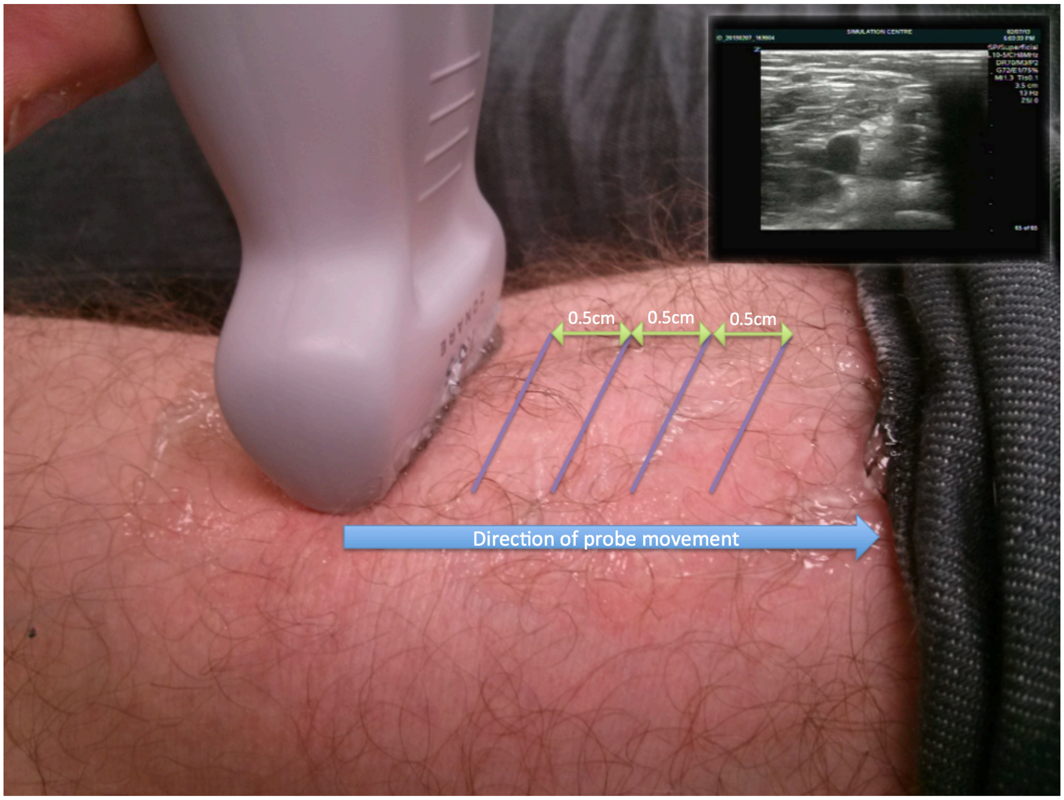

Fig. 29: Illustration of probe placement and movement for ultrasound nerve block. The arrow shows the direction of probe movement during the study. The picture in picture (top right) represents the display of the ultrasound with the probe in this position.

For the femoral nerve, in part I of the study, 6 participants are imaged bilaterally using the standard ultrasound guided nerve block procedure for the femoral nerve. The probe is moved cranially and caudally in increments of 0.5 cm from 2 cm below the inguinal ligament to capture 10 images per side for a total of 120 images over the 6 participants. Images are captured when the anaesthesiologist can see the nerve within the image. In part II of the study, the video analysis component, videos are captured from 4 participants in the same manner as part 1, moving the probe cranially and caudally increments of 0.5 cm, pausing for 5 to 10 seconds at each increment once the nerve could be seen within the ultrasound feed. Videos are recorded as long as moving the probe still allows the anaesthesiologist to visualize the nerve. Each participant's legs are imaged twice. In part III of the study, the decision support component is tested on 2 participants imaged bilaterally. The anaesthesiologist is asked to follow the protocol given by the NerveGPS exactly to try and detect the nerve.

5. 1. 1. 2. Evaluation of results

For part I of the study, the algorithm is evaluated by determining the overlap between the software detected nerve center and an area manually identified by an experienced anaesthesiologist as the nerve. An anaesthesiologist determines the manually detected area. The anaesthesiologist then draws the contour of the nerve in the image if the nerve is present within the image. To determine overlap, the algorithm is run on the images to obtain the software detected nerve center. Concentric circles are drawn around the nerve center as seen in Figure 30. Concentric circles are chosen to emulate the shape of Tuohy needle tip. Overlap is calculated for concentric circles of increasing diameter and is defined as the ratio of the union of the manually detected area and the circle to the manually detected area:

$$Overlap = \frac{Manual \cup Circle}{Manual}$$

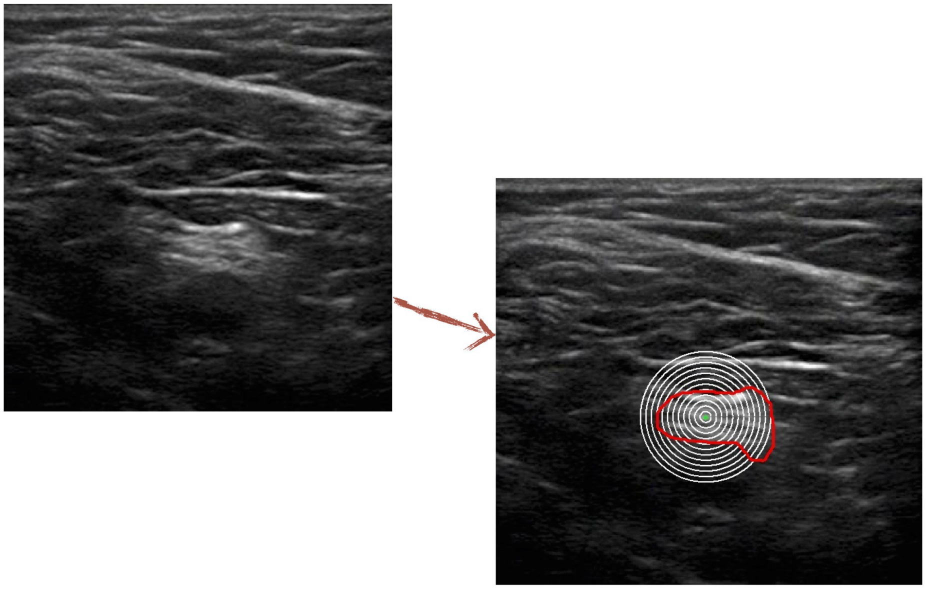

Fig. 30: Illustration of evaluation methods. The center point of the concentric circles corresponds to the software detected nerve center and the red contour corresponds to the manually detected nerve area.

Figure 31 illustrates the overlap evaluation method. The overlap percentage is 100% when the concentric circle is entirely contained in the manually detected area.

For the video analysis component of the study (part II), videos were evaluated by calculating the ratio of the amount of time where the nerve was detected to the amount of time the nerve was actually within the image. The number and length of erroneous detections was also recorded.

To test the decision support system (part III), the results were based on the answer to the question:

> Did the instructions provided by the NerveGPS decision support system allow for the detection of the nerve using the automated nerve detection function?

If the anaesthesiologist agreed with the detection at the end of part III then 'Yes' was recorded.

Circle diameter (mm)	Overlap Percentage
1	100%
2	100%
3	100%
4*	100%*
5	100%
6	100%
7	98%

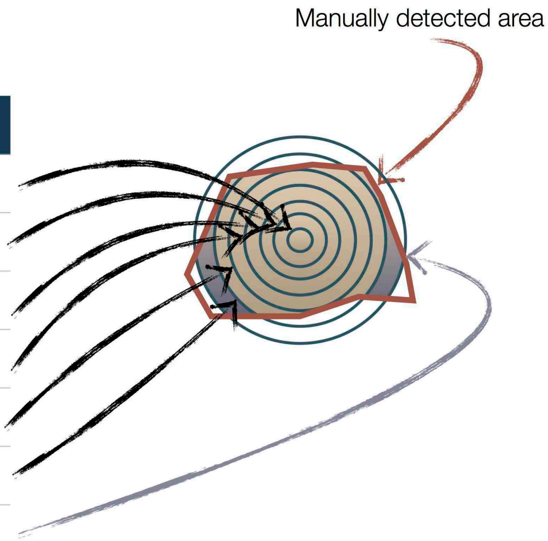

Fig. 31: Illustration of overlap evaluation method

5. 1. 1. 3. Analysis

To determine the clinical significance of the results, we set a clinically significant goal for each of the study parts. The clinically significant diameter for overlap was set at 0.4cm. Distances above 0.4cm were considered at risk of an unsuccessful block. For other parts, clinical significance of the detection was established at the discretion of the anaesthesiologist evaluating the performance of the software.

5. 1. 2. Results

5. 1. 2. 1. Part I results: Image analysis

The results for part I of the study for the popliteal and femoral nerves are displayed in tables 3 and 4 respectively. For the popliteal nerve, the nerve center was within the manually defined area in 100% of the cases. The overlap for the 4mm diameter circle, the minimum clinically significant diameter, was 98%. For 7mm diameter the overlap was of 88%.

Circle diameter (mm)	Mean
1	100%
2	100%
3	99%
4*	98%*
5	95%
6	92%
7	88%

Table 3: Average nerve detection overlap for the sciatic nerve at the popliteal fossa

For the femoral nerve, the software-detected nerve center was within the manually defined nerve center in 84% of the cases (101/120 images). The femoral nerve detection uses an additional parameter for scoring: the distance from the artery. Since the nerve is always lateral to the artery, an ideal distance from the artery was defined for the nerve center using the data from 40 extra images. The closer the nerve center was to this ideal point, the higher the distance score. The 19 images in which the nerve was not in the center, the artery was not properly detected. Issues with artery detection are usually not present when dealing with live video. When using video feeds the additional support of the color Doppler, which clearly highlights the location of the vessels, can be used. Removing the errors that arise when the artery is not properly located, the nerve center is located in the manual area in 100%

of cases. For a circle of diameter 4mm, the overlap between the automatic detection and manual areas is of 82%. This can be approximated to 97-98% when adjusted or the error in vessel detection.

Circle diameter (mm)	Mean
1	84%
2	84%
3	83%
4	82%
5	79%
6	76%
7	73%
8	68%
9	64%
10	59%
11	54%
12	50%

Table 4: Average nerve detection overlap for the femoral nerve

5. 1. 2. 2. Part II results: Video Analysis

The results for part II of the study for the popliteal and femoral nerves are displayed in tables 5 & 6 respectively. For the popliteal nerve, the nerve was detected on average 89% ± 8% of the time in the videos, with average detection times for each video ranging from 80% to a high of 98%. Videos ranged between 240 and 360 seconds in length. When the software erroneously detected an area after an iteration of the algorithm, the erroneous detection usually lasted for short periods of 1 or 2 seconds in 73% of the cases. The algorithm took on average 451ms to run with times ranging from 305ms to 832ms.

Length of erroneous detection (s.)	1	2	3	4	5	6	7	8	9	10	10+	Total	%
RK (254 s.)	2			1								6 s.	98%
MG (260 s.)	3	8		1	1			1				36 s.	86%
CP (360 s.)	12	5	1		1		1	1			2	71 s.	80%
JM (300 s.)	8	3	1	1								21 s.	93%
MW (240 s.)	1										2	31 s.	87%
SC (360 s.)	2	2	1	1	1							18 s.	95%
Average												89% ± 8%	

Table 5: Video detection results for the sciatic nerve at the popliteal fossa on 6 subjects.

For the femoral nerve, the software was tested on 4 participants. The results were expressed as the percentage of successful detections rather than the percentage of time where the nerve was successfully detected. The average detection time for the femoral nerve was of 87%, with detections ranging from 68% to 98% on average for each participant. Results varied from one leg to another. Occasionally, for certain participants, significantly different detection rates could be observed between consecutive scans of the same leg. For "RK left" as can be seen in Table 6 for example, the first scan was unable to detect the nerve, whereas the second scan detected the nerve in 71% of detections. These differences were often due to difference in probe tilt.

Dashes were used to indicate videos in which the nerve could not be successfully detected manually by an anaesthesiologist.

Duration during which nerve was successfully detected (%)	Left		Right		Total
	1	2	1	2	
SC	90	100	100	100	98%
TH	100	100	82	100	96%
RK	0	71	100	100	68%
MG	97	61	-	100	86%
Average					87%

Table 6: Video detection results for the femoral nerve

5. 2. Part III results: Decision support testing

When integrated into the decision support system, the nerve location is represented by the red circle seen in Figure 12. The location is determined by the results from the algorithm. The result of every detection is recorded and the frequency of detection at every point is displayed in the heat map in the image frame of the GUI. The area that has the highest frequency of hits (red in the heat map) is determined to be the nerve area. A successful detection occurs when the instructions given by the NerveGPS decision support system lead to the detection the nerve using the nerve detection algorithm.

Tables 7 and 8 represent the results from using the full NerveGPS decision support system for the popliteal and femoral nerves respectively. For the popliteal nerve, either the tibial and peroneal or sciatic nerve was detected for both participants on both legs. The sciatic nerve was detected in 3 out of 4 cases and the tibial or peroneal was also detected in 3 out of 4 cases. In each case, one of either the tibial/peroneal or sciatic nerve was detected. When the NerveGPS failed to see the sciatic nerve using software, the tibial or peroneal nerves were detected. In the case where the tibial or peroneal weren't detected, the sciatic nerve was.

Nerve		Tibial or Peroneal Nerve	Sciatic Nerve
Participant 1	Left	Yes	Yes
	Right	No	Yes
Participant 2	Left	Yes	Yes
	Right	Yes	No

Table 7: Results of NerveGPS use for the sciatic nerve at the popliteal fossa

For the femoral nerve, the instructions given by the NerveGPS allowed for detection of the nerve 100% of the time when 2 patients were imaged bilaterally.

Nerve		Femoral
Participant 1	Left	Yes
	Right	Yes
Participant 2	Left	Yes
	Right	Yes

Table 8: Results of NerveGPS use for the femoral nerve

• Chapter 6 – Discussion

6. 1. Discussion

Residents and clinicians that wish to complement their residency training in regional anaesthesia sometimes seek 12-month fellowship. During this fellowship, anaesthesiologists undergo an academic course covering the anatomy, techniques, and complications of regional anaesthesia and a practical portion to acquire the needed psychomotor skills (Hargett et al., 2005). Regional anaesthesia fellowship training like much of the current medical training, is based on the maxim "See one, do one, teach one". Although this rule has been applied successfully to many of the tasks required from physicians, assistive tools could potentially make the practice safer, more efficient and more effective. Ultrasound guided regional anaesthesia requires bi-manual dexterity to hold the probe in one hand and guide the needle through to the nerve with the other. The anaesthesiologists are comfortable with the anatomy of the region and the tools they use to follow the needle through the skin. Mastery of these cannot prevent complications that arise even when the procedure is done perfectly. Assistive tools could potentially help improve the safety and efficiency of the procedures.

One of the ways safety can be improved is through the use of simulation phantoms or mannequins. High-fidelity mannequins can be used to practice and acquire the psychomotor skills necessary for ultrasound guided nerve block. Currently, phantoms developed by Blue Phantom (CAE Healthcare, Sarasota, FL, USA) facilitate the practice of psychomotor skills of nerve localization and needle insertion (Figure 32 & 33). The phantom consists of a gel with 3 hyperechoic structures (1 superficial and 2 profound) and 1 liquid filled structure representing a vessel. While this phantom can be helpful in the earlier stages to get acquainted with the ultrasound platform and obtain some of the psychomotor skills needed, it does not accurately present the physician-in-training with the challenges of ultrasound image interpretation for nerve localization and needle tip visualization. The NerveGPS could help bridge the gap between the academic knowledge of the sonoanatomy and its practical interpretation. The NerveGPS could be used as part of the training procedure for nerve localization. Trainees could take turns scanning each other using the ultrasound probe for different blocks using the instructions provided by the NerveGPS. The instructions provided by the decision support system would provide them with the information necessary to place the probe at the correct location. Once at the correct location, the automated nerve detection software could be activated to confirm or indicate the location of the nerve to the user. This could be extended for use on actual patients as well.

Fig. 32: Ultrasound probe placed on an ultrasound nerve block training phantom (BluePhantom, 2013)

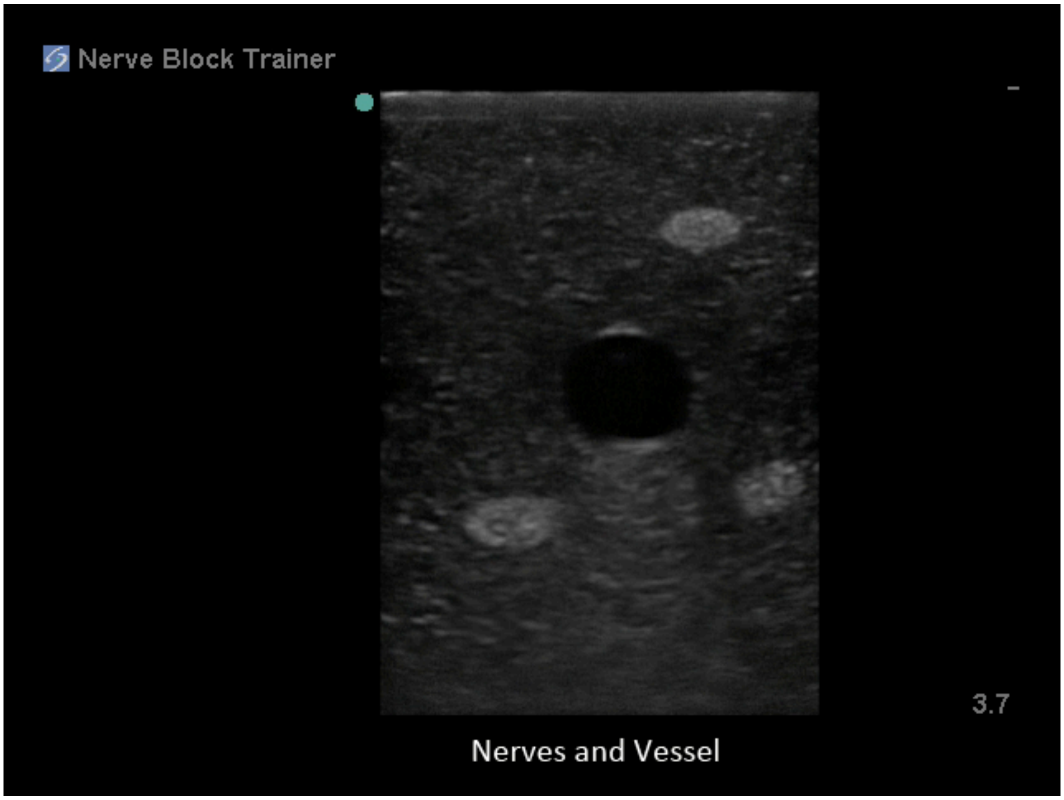

Fig. 33: Ultrasound image obtained by placing an ultrasound probe on the ultrasound nerve block training model as seen in Figure 32. (BluePhantom, 2013)

In a similar manner to which the NerveGPS can be used as a training tool, anaesthesiologists can use it to obtain a second opinion when trying to locate the nerve. Anaesthesiologists are expected to perform a large variety of tasks, some more often than others. The instructions provided by the NerveGPS could serve as a refresher when performing less common nerve blocks – procedures that the anaesthesiologists may be slightly less familiar and comfortable with. It could help standardize the procedure.

The NerveGPS features several limitations. The testing and studies performed for the system were suitable for the purposes of a feasibility study, however more information could be obtained by knowing the recall of the image-processing algorithm. Due to the limited amount of images, tests could not be adequately performed to calculate recall otherwise known as specificity, a measure of the software's accuracy at excluding false positive's. To calculate recall, the software could be tested on N amount of images of the region of interest where the nerve is visible and N amount of images of the region of interest where the nerve is not visible. The results from the latter test will give the image processing algorithm's recall.

Moreover, the software in its current state is only suitable for 2 nerves: the femoral and popliteal nerves. These nerves are similar in shape and texture: oval or triangular shaped with a honeycomb texture. Other nerve block areas such as the plexus brachialis, where a network of nerves can be seen in the ultrasound image, present a different challenge and would require a different approach to the image processing algorithm.

The evaluation methodology to determine the overlap between the manually defined nerve area and the software detected area was ill-suited for this application. The concentric circles methodology described in section 5.1.1.2 was initially selected for its simplicity and the assumption that the nerve is oval shaped. This method however fails to show a representative overlap for larger circles when the nerve is oval shaped and larger distances separate its foci. Figure 31 illustrates the limitation in the concentric circles methodology used. In Figure 31 the leftmost pane represents the ultrasound image without markings, the middle pane the ultrasound image with markings corresponding to the manually detected nerve area in red, the software determined nerve center in green and the concentric circles used for overlap in white. The rightmost pane is a table representing the results of the overlap for this nerve. The middle pane shows that the nerve center was detected right in the center of the manually detected area. This should in theory give us perfect overlap for all circles. The overlap however is 100% for circles from 1 to 5mm and decreases from 6mm on. This shows that the evaluation method is only reliable for small circles up to approximately 5mm. This was suitable for the pilot study since the minimum clinically significant diameter was set at 4mm. Future implementations should shift to segmentation coverage to better represent the overlap between the 2 areas. Segmentation coverage would use the nerve boundaries found using Chan-Vese active contours and compare them to the manually detected area, for a more accurate representation of overlap. The clinical significance could be further improved by injecting a short acting local anaesthetic to validate the process.

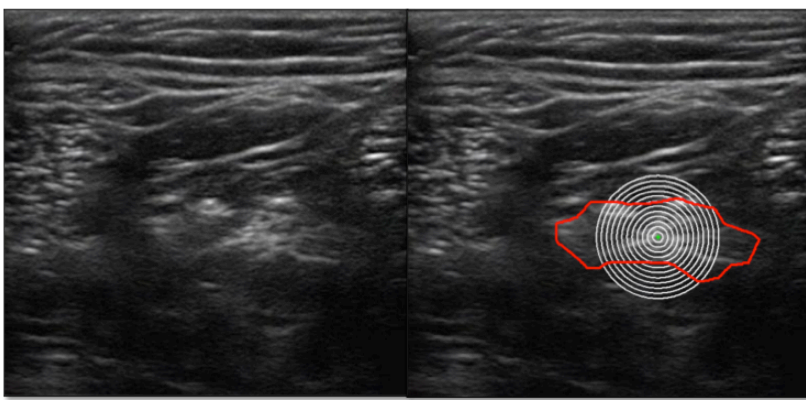

Circle diameter	Overlap Percentage
1.0 mm	100%
2.0 mm	100 %
3.0 mm	100 %
4.0 mm	100 %
5.0 mm	100 %
6.0 mm	97 %
7.0 mm	92 %
8.0 mm	86 %
9.0 mm	80 %
10.0 mm	74 %

Fig. 34: Limitations of the evaluation method used to determine overlap between the manual and automated nerve detections.

The algorithm was also limited by the small dataset available for development. Techniques with a faster runtime that may be more accurate and reliable include machine-learning techniques such as artificial neural networks. These techniques require a large set of images to train the neural network. The large set of images would also allow a more scientific approach to the number of detections needed to get an accurate location from the

NerveGPS. The NerveGPS could then provide the user with the degree of confidence with which they believe the detected area corresponds to the nerve.

The decision support system aspect of the NerveGPS also features several limitations. The current system only provides the instructions for certain approaches to a nerve block. The instructions for the sciatic nerve at the popliteal fossa for example only provide instructions for performing the procedure with the patient in a prone position. This position however is not always optimal for performing the nerve block, and other positions can be favoured. Improved versions of the software should take different positions into consideration. Adapting the software for a lateral approach should be relatively simple given that the lateral approach provides the same sonoanatomy rotated by 180°.

The ultrasound platform and the decision support system currently run on two different machines. The dissociation between the ultrasound platform and the computer used to run the NerveGPS make using the latter cumbersome and unintuitive. The current setup allows the user to follow the display of the ultrasound feed on the computer however it does not allow the user to access essential functions of the ultrasound platform activating and deactivating Doppler and changing the depth of the ultrasound probe. To improve the usability of the software, the decision support system should be integrated into the ultrasound machine. Unfortunately the current ultrasound platforms cannot be modified to display the NerveGPS. The ideal setup would be using the Sonosite X-Porte.

The NerveGPS has a very long load time on start up. The NerveGPS software takes approximately 20 seconds to load the MATLAB scripts. Using a lightweight alternative computer vision library like OpenCV can reduce the significant overhead of loading MATLAB. In addition, the use of OpenCV could optimize runtime by allowing increased parallelization of segments of the algorithm.

6. 2. Future Work

Future development should focus on expanding the software to other regions of interest for ultrasound guided nerve block. One such area that has been researched for automated application is the plexus brachialis. The plexus brachialis can be blocked using one of several approaches. Preliminary tests are being conducted to determine the feasibility of the NerveGPS for the plexus brachialis with the supraclavicular approach. The nerve at this area presents a significant challenge due to its close proximity with the lungs. An erroneous detection in this area for example could guide the user to insert the needle too far and cause a pneumothorax.

Future work will also focus on creating a database of ultrasound images for the regions of interest from volunteers to use these in machine learning applications. Two plans have been devised to fill this database: collecting images from volunteers that are image solely for the database or partnership with a hospital to collect and save images obtained during ultrasound courses or even ultrasound guided nerve block interventions. The database will allow for a diverse range of images, visualized at different depths and on participants with different anatomies, to further improve the NerveGPS by integrating machine learning.

6. 2. 1. Robotic applications

The NerveGPS system is designed in part to fit into the Magellan system for automated nerve block (Joshua Morse, Wehbe, Taddei, Cyr, & Hemmerling, 2013). The Magellan system would consist of one or several robotic arms that would attend to the mechanical portions of the procedure: needle insertion and probe movement. Pilot testing has already successfully been conducted on phantoms (J Morse et al., 2014) and humans (Thomas M Hemmerling et al., 2013) to perform the needle insertion portion of robot-assisted ultrasound guided nerve block. This procedure was performed using a JACO robotic arm by KINOVA (Montreal, QC, Canada) as seen in Figure 35. The proposed Magellan system would feature 2 software components, one for the localization and movement of the arms and one for the localization of the nerve. The NerveGPS algorithm would locate the nerve. Research is also being conducted to include the NerveGPS with a needle driver attached to an ultrasound probe. A handheld ultrasound probe and needle driver would free up one of the hands of the anaesthesiologists. The Magellan system would be designed to complement the anaesthesiologist by performing some of the more precise mechanical tasks and allowing the anaesthesiologist to focus on patient monitoring and reduce the risk of complications.

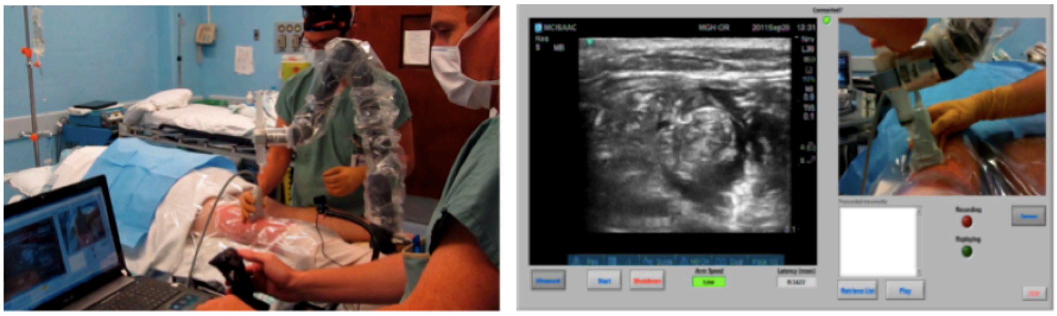

a) b)

Fig. 35: Views of the Magellan robot assisted ultrasound-guided nerve block (Thomas M Hemmerling et al., 2013). In a) a view of the arm being used on a patient and b) the cockpit view.

6. 2. 2. Robotics in medicine and anaesthesia

The Magellan robotic nerve block system would come to complement existing robotic and mechanical systems being used in the medical field. The goal of surgical robots is to provide less invasive techniques and eventually create the possibility of teleoperation to provide care to remote parts of Canada and the world. These systems can be divided into 2 categories: image guided robots and surgical robots. Image guided robots are the least prevalent systems in use. These systems are fed a set number of images on which the robot will take action to perform a simple operation. Two such systems are the Acrobot (M. Jakopec, 2003) and Robodoc (R. H. Taylor, 1999). Another system, developed by (Hong, Dohi, Hashizume, Konishi, & Hata, 2004), uses ultrasound to drive a needle insertion robot for percutaneous colecystotomy.

Among surgical robots, the Da Vinci robot stands out as one of the most prominent robots. The Da Vinci robot is a teleoperated robot that mimics the motions of the surgeon's hands, allowing for greater precision during surgery. The Da Vinci currently has over 2200 systems in use with over 360 000 procedures performed in 2011 using the system (Hannaford et al., 2013). The Da Vinci is also one of the best examples to demonstrate the advantages of surgical robotics. The system was shown to reduce complications during intestinal (S. J. Marecik, 2007) and oesophageal surgery (S. Horgan, 2005). The Da Vinci provides improved dexterity during laparoscopic surgery and has been privileged during nerve-sparing radical prostatectomy (Ahlering, 2006). The Da Vinci's disadvantages impede its more widespread adoption. The robot is a costly tool that has a significant learning curve. Other teleoperated robots have been developed, notably a system for tele-echography (Vilchis, Troccaz, Cinquin, Masuda, & Pellissier, 2003). The surge in interest in surgical robotics is illustrated by the development of the Raven II, an open source platform for surgical research (Hannaford et al., 2013). Unlike the Da Vinci system, the Raven II is not robust enough to be used in humans although it has been used for repeated experiments and animal surgery experiments. The Raven II platform aims to provide hardware and software that can be used by teams for reliable, repeated and sustained surgical experimentation. The components are built using as much transparency and open source tools as possible to promote sharing and the growth of the robotic surgery experimentation field. All software development is done using Linux and ROS to facilitate software development and the use of the tool by other teams for surgical experimentation. The Raven II, much like the Magellan, aims to integrate intelligent and computational task into the robotic procedure.

A team at the University of British Columbia developed the robot most similar to the Magellan. Their system aimed to use images obtained from an ultrasound feed, a robotic controller and a robotic arm to control ultrasound probe movement in certain areas and prevent the clinician from having to hold the probe in an awkward position for long hours (Abolmaesumi et al., 2002).

Chapter 7 – Conclusion

Current research in medicine has focused on improving devices and providing clinicians with tools to improve patient safety and reduce the cost of procedures. Tools to support clinicians in their decisions are becoming more prevalent and accepted and the benefits of these tools are becoming clearer. Despite the growth of research in this field and its apparent benefits, few systems are currently in use today.

The purpose of this thesis was to demonstrate the feasibility of a decision support system with an integrated tool for automated nerve detection to potentially improve the training, adoption, success and difficulty of ultrasound guided nerve block.

The decision support system complements existing functions of the ultrasound platforms in use in operating rooms. The system provides the user with a full set of instructions on the settings, probe placement and probe movements needed to determine the area of interest for regional nerve blockade. The system can then detect the nerve using an automated nerve detection algorithm developed using image processing tools. Both the full decision support system and the automated nerve detection system have been tested and have provided positive and consistent results in pilot studies using different types of media. During still image analysis the nerve is located in 99% and 83% of the cases for the popliteal and femoral respectively. Video analysis yielded equally positive results, providing similar detection accuracy in addition to validating the software's suitability for real-time analysis with a runtime of 451ms on average. Finally, testing of the decision support system validated its capability to provide the full set of instructions necessary to locate the nerve.

The work done in this thesis demonstrates the feasibility of a decision support system for ultrasound guided nerve block. The instructions can be used for training purposes and the automated detection software for providing clinicians with a second opinion. This work goes towards the improvement of anaesthesia processes and nerve block procedures. The application of this system to real-life situations can hopefully improve the quality of patient care in the future.

Appendix 1 – IEEE proceeding: "Nerve GPS: A novel decision support system for ultrasound nerve block guidance"

Presented at 'IEEE Computer Based Medical Systems' Conference on May 27th 2014.

With sponsorship from the Society of Technology in Anesthesia's Fresenius Grant

Abstract

Peripheral regional nerve blockade (nerve block) is used in anesthesia to administer anesthesia to certain regions of the body. During nerve block the anesthetic is injected directly into or around the area surrounding the nerve. One of the most critical components of ultrasound-guided nerve blocks is the detection of the nerve within the ultrasound image. This study presents a software-based solution for the detection of nerves within the ultrasound feed. The software that was developed used image processing tools to detect the location of the sciatic nerve at the popliteal fossa within an ultrasound feed. For the study, 100 images were obtained from authors. Then, 2 anesthesiologists with experience in ultrasound-guided nerve blocks were asked to identify the contour of the nerve in the obtained images. The study used two criteria for evaluating the software: 1) the location of the software determined nerve center fell within the manually defined contour and 2) the percentage of overlap between the software and manually detected areas. A test was successful if the percentage of overlap between automatic and manual detection was a minimum of 95% for a circle of 0.4cm diameter

centered at the software detected nerve center. For the 100 image sample, the nerve was detected within the manually detected area in 99% of the cases, with an overlap of 98% for a 0.4cm diameter circle. Time to detect the nerve ranged from 0.95s to 1.6s. These preliminary results show that the nerve detection software provides a reliable target for needle insertion. Future work will extend the software to different nerves of interest.

Keywords—ultrasound; decision support; nerve block; sciatic nerve; ultrasound imaging

I. INTRODUCTION

Peripheral regional nerve blockade is used to administer anesthesia to a sizable portion of the body. There are 2 principal components to regional anesthesia: 1) the interpretation of the sonoanatomy and identification of the neural components, and 2) the insertion of the needle and injection of the anesthetic into the previously identified area.

The interpretation of the sonoanatomy and the correct identification of the neural components are critical to the success of the peripheral nerve block procedure. Injection of the anesthetic outside of the area surrounding the nerve may result in an unsuccessful block. The identification of the nerves within ultrasound images is however difficult (Tsui & Finucane, 2006).

Consequently, ultrasound-guided interventional procedures in regional anesthesia require an advanced knowledge of ultrasound systems usually acquired over the course of a fellowship and extensive experience (Narouze et al., 2012). Current technologies to aid with ultrasound-guided nerve blocks have focused on improving the visibility of the needle within the ultrasound image. To improve visibility, existing echogenic needles feature echogenicity-enhancing features in the materials and textures used that enhance the brightness and clarity of the needle (Sviggum, Ahn, Dilger, & Smith, 2013). More recently, the Enhanced Needle Visualization (ENV) or Multibeam enhancement (MBe) software upgrade advertised by Sonosite (Bothell, WA, USA) was developed to help discern the needle position within the ultrasound image. At present, the Doppler ultrasound is one of the only technologies that offers a visual overlay of elements of the sonographic anatomy on the ultrasound system's display. The use of pulse-waved color Doppler technology to identify vessels and regions of blood flow within the ultrasound image can help prevent complications during regional anesthesia (Falyar, 2010). However, all technological advancements have focused on a better visualization of the nerve block needle, but none on the autonomous detection of the nerve, which would be of great aid to anesthesiologists.

The following paper presents the initial version of software for the detection of neural components within an ultrasound image, software capable of detecting the sciatic nerve at the popliteal fossa within an ultrasound image.

II. BACKGROUND

A. Ultrasound

Ultrasound machines are non invasive medical devices used to image various areas of the body. These devices use a transducer that emits high frequency sound waves into the regions of interest. The echo of the sound waves off structures within the body are interpreted by the ultrasound platform to build the ultrasound image. Inherent to ultrasound is the presence of speckle noise, a random pattern of interference specks. Speckle noise degrades the quality of the image and complicates the evaluation of the sonoanatomy (Pizurica, Philips, Lemahieu, & Acheroy, 2003). The suppression of speckle noise, without compromising elements of the image that are useful for medical evaluation is a well researched field that currently offers many solutions for image processing applications.

B. Nerve block

Peripheral nerve blocks are a method of administering anesthesia to a region of the body through injection into the nerve or the area directly surrounding the nerve. Peripheral nerve blocks are used for surgical anesthesia or postoperative pain management. Peripheral nerve blocks are often used when performing an operation on a limb, and are preferred over general anesthesia when possible.

There are two different methods for performing nerve block: landmark based nerve stimulation and ultrasound guidance. During electrical nerve stimulation, the anesthesiologist uses an insulated needle to provide a short, low intensity electrical stimulus to solicit a response from the patient and locate the position of the nerve. Ultrasound guidance is a more complex procedure where the anesthesiologist will have access to the sonoanatomy of the area of interest and look to interpret this sonoanatomy to locate the nerve. It provides a more efficient, less invasive and more secure method than nerve stimulation. Nerve stimulation often requires the use of a larger volume of local anesthetic to increase the chance of block success when compared to ultrasound guidance (Casati et al., 2007). During procedures on patients with a difficult anatomy, or when the anesthesiologist is less experienced with ultrasound guided nerve block, a combination of ultrasound guidance and peripheral nerve stimulation is used. The ability to view the patient anatomy with ultrasound guidance gives it a significant edge over nerve stimulation (Nowakowski, Bierylo, Duniec, Kosson, & Lazowski, 2013; Orebaugh, Bigeleisen, & Kentor, 2009). An improvement to the tools used for ultrasound guidance could decrease the complexity and increase the success of the procedure.

III. METHODS

This study was performed for the identification of the sciatic nerve at the popliteal fossa using a posterior approach with the patient in a prone position. An ultrasound experienced anesthesiologist imaged the authors at the popliteal fossa, using a water based conducting gel and a high frequency (>7MHz) linear array ultrasound transducer (Zonare L8-3 Linear Array transducer and Sonosite L38 transducer) attached to an ultrasound machine (Zonare z.one ultrasound platform and Sonosite MicroMaxx). 100 images were obtained bilaterally from 5 authors by moving distally from the popliteal fossa, in increments of 0.5 cm (10 per side) until the bifurcation into the tibial and peroneal nerves (Fig. 1 & 2), to image the nerve at different locations. The nerve was present in all ultrasound images. All authors were of healthy weight with a body mass index between 18.5 and 24.9.

A. Setup

The ultrasound feed was taken from the machine's HDMI output port and connected to the computer using a video composite to USB frame grabber with a maximum resolution of 640x480. Image capture would begin once the anesthesiologist operating the probe identified the nerve of interest. For each author, ultrasound images of the nerve were taken at the same depth setting. Acquired images were taken without the use of color Doppler.

B. Filtering methods

The acquired images were sorted by date and participant for testing. Once loaded, the unmarked image is resized to feature only the regions of interest. The image is then fed through a wavelet transform filter to reduce the ultrasound speckle noise. A single level discrete 2-D wavelet transform was used, with a high-low (HL) filter pair. Filter pair selection was done using a black-box methodology with MATLAB's (MathWorks, Natick, MA, USA) wavelet 2-D tool. K-means clustering, an iterative clustering algortihm is used to divide the image into 5 different layers based on pixel intensity. The intensity layers were then eroded using 3 different structuring elements to separate large objects connected by only a few pixels.

The anatomical properties of the sciatic nerve at the popliteal fossa were then used for its identification. The nerve's two most distinctive anatomical properties are its hyperechoicity and oval shape. Using these properties, objects on the 3 highest intensity layers are run through a scoring algorithm that assigns them a score based on 4 different criteria (listed in order of weighted importance):

- Area.
- Eccentricity
- Height-to-Width ratio. This will eliminate the long, thin and hyper echoic strands that usually represent muscle fascia.
- Intensity

The weights of the scoring algorithm were based on analysis of the manual detection of the nerve area by anesthesiologists. For each image, properties of the manually identified regions of interest (i.e., area, perimeter, equivalent diameter, bounding box and mean intensity) were extracted and aggregated. The collected data was analyzed to find the properties with the lowest coefficient of variation. Weights were determined based on the coefficient of variation, with importance inversely proportional to the coefficient of variation. To ensure that the software achieved high specificity, extrema thresholds were set at 2 standard deviations from the mean for each property individually. A threshold of the lowest score for an object with traits consistent with a nerve was set. The center of the object with the highest score is returned to the user as the suggested center of the nerve. If none of the scores exceed the threshold, it is assumed that the image does not contain the nerve.

C. Evaluation of results

An overlap area based approach was taken for the evaluation of the software. The 2 criteria that were used to determine the software's success were: 1) the successful identification of the nerve and 2) its location at least within a 0.4cm diameter from the inside of the nerve. To evaluate the precision of the software detected nerve, two ultrasound experienced anesthesiologists were asked to manually identify the boundary of the nerve within each ultrasound image. Concentric circles of incremental diameter were then drawn around the software's detection of the nerve center in 0.1cm increments from 0.1cm to 1cm in diameter. The manually identified area (*Manual*) was compared to each circle (*Circle*) using (1) to determine the overlap (Table 1).

$$(Manual \,\&\, Circle) \,/\, Manual = Overlap \quad (1)$$

The quality of the image showed a direct correlation with the speed at which analyses could be performed. Detection times ranged from 0.95s to 1.69s.

IV. DISCUSSION

We developed software for the identification of the sciatic nerve at the popliteal fossa within ultrasound images. The system used image processing to determine the location of the center of the nerve. The system proved reliable in determining the center of the nerve in 99% of the ultrasound images and produced an overlap of 98% for a 0.4 cm diameter circle. Given that the standard outside diameter of a Tuohy needle ranges from 0.8mm to 1.1mm, the 0.4cm diameter target can be seen as a clinically sufficient target area for nerve block needle placement to allow sufficient injection of anesthetic into the nerve. This allows for a margin of error of 0.3cm.

Several technologies exist that help anesthesiologists identify elements of sonographic anatomy. The Doppler ultrasound is a decades old scanning tool that helps identify the regions of blood flow within an ultrasound image. At present, the use of the Doppler as a performance and verification tool is recommended in many types of ultrasound-guided operations and proficiency with the tool is required for ultrasound-guided pain medicine procedures, including nerve block (Narouze et al., 2012). One of the errors that arise most commonly during ultrasound-guided nerve blocks is the advancement of the needle without visualization (B. D. Sites, J. D. Gallagher, J. Cravero, J. Lundberg, & G. Blike, 2004; Sites et al., 2007). Among the technological solutions to this common issue are echogenic Sneedles or the Enhanced Needle Visualization (ENV) or Multibeam enhancement (MBe) software advertised by Sonosite (Bothell, WA, USA) for their M-Turbo® and S Series™ ultrasound machines to improve the visibility of the needle in the ultrasound image. This software has the potential to make operations involving ultrasound safer thanks to the enhanced visibility of the needle(Takatani et al., 2012). Similarly, the automated ultrasound nerve detection could give the anesthesiologist a tool to complement the existing technology by locating the position of the nerve.

The study design features certain limitations. The ultrasound images used for the study were taken from authors having a similar anatomy and a healthy weight with a body mass index between 18.5 and 24.9. A more complete study would feature participants with more diverse anatomies. The study tested the capability of the software to detect the sciatic nerve at the popliteal fossa within an ultrasound image. The study however did not feature images in which the nerve was not present. Finally, the software evaluation method described in the method section, based on the overlap between manual and software detection, is often not appropriate for circles of diameter superior to 7mm. This method was however appropriate for this study since the region of interest for reliable needle insertion was set at 0.4cm.

Future work will focus on the development of an algorithm for other nerves of interest and the real time applications of the software. In the long term, we hope to pair the software's capabilities with the Magellan robotic nerve block system (T. M. Hemmerling et al., 2013) to perform fully-automated ultrasound-guided nerve blocks.

Figures

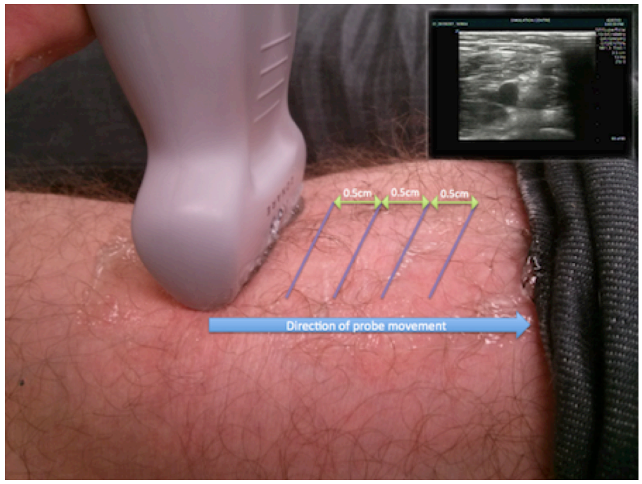

Fig. 1 – Illustration of probe and needle placement for ultrasound nerve block at the popliteal fossa. Arrow indicates the direction of probe movement used for image capture during the study.

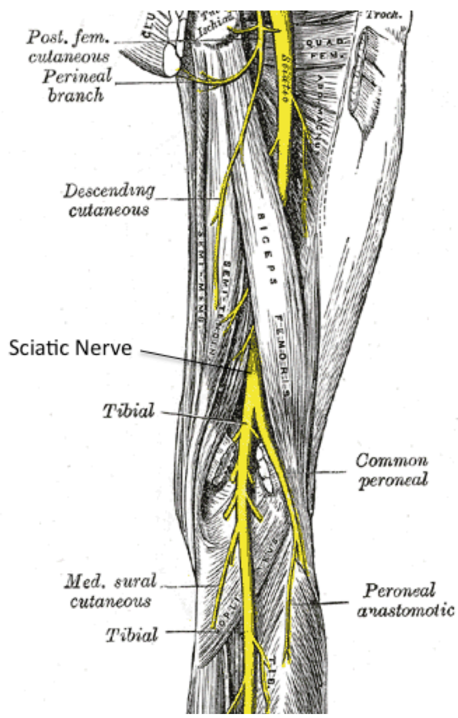

Fig. 2 – Anatomical view of the neural components surrounding the sciatic nerve at the popliteal crease, adapted from (H. Gray, 1918)

(a)

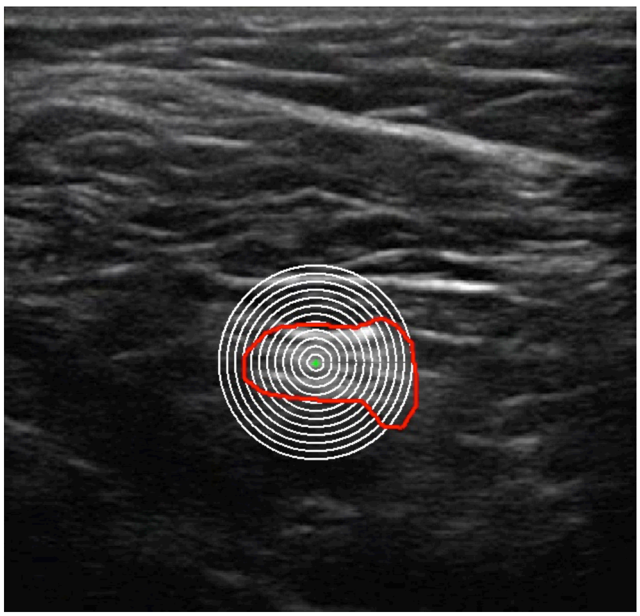

(b)

Figure 3 - Ultrasound image of the sciatic nerve at the popliteal fossa at a depth of 4 cm: a) before software detection of the nerve and b) after software detection of the nerve. In b), the red line corresponds to the manually defined boundary, the green dot to the center of the nerve as identified by the software and the white circles are used to determine the overlap of the software and manual detections. Adjacent white circles differ by 0.1cm in diameter.

Table 1 – Software nerve detection Results

Average Nerve Detection Results	
Circle diameter (mm)	Overlap Percentage
1	100 %
2	100 %
3	99 %
4[a]	98 %[a]
5	95 %
6	92 %
7	88%

*Minimum clinically significant circle diameter

LIST OF REFERENCES

Abolmaesumi, Purang, Salcudean, Septimiu E, Zhu, Wen-Hong, Sirouspour, Mohammad Reza, & DiMaio, Simon Peter. (2002). Image-guided control of a robot for medical ultrasound. *Robotics and Automation, IEEE Transactions on, 18*(1), 11-23.

Ahlering, T. E. (2006). Robotic prostatectomy: Is it the future?,. *Urolog. Oncol., 24*, 3.

Anderson, Martin E, & Trahey, Gregg E. (2000). A seminar on k-space applied to medical ultrasound. *Course Notes for use in BME, 265*.

Anesthesia, New York School of Regional. (2013, 20/09/2013). Femoral Nerve Block. from http://www.nysora.com/techniques/nerve-stimulator-and-surface-based-ra-techniques/lower-extremitya/3267-femoral-nerve-block.html

Bigeleisen, Paul E. (2006). Nerve Puncture and Apparent Intraneural Injection during Ultrasound-guided Axillary Block Does Not Invariably Result in Neurologic Injury. *Anesthesiology, 105*(4), 779-783.

BluePhantom. (2013). Regional Anesthesia Ultrasound Training Block Model. from http://www.bluephantom.com/product/Regional-Anesthesia-Ultrasound-Training-Block-Model.aspx?cid=525

Bodenham, A. R. (2006). Editorial II: Ultrasound imaging by anaesthetists: training and accreditation issues. *British Journal of Anaesthesia, 96*(4), 414-417. doi: 10.1093/bja/ael032

Borgeat, Alain. (2006). Regional Anesthesia, Intraneural Injection, and Nerve Injury: Beyond the Epineurium. *Anesthesiology, 105*(4), 647-648.

Casati, A., Baciarello, M., Di Cianni, S., Danelli, G., De Marco, G., Leone, S., . . . Fanelli, G. (2007). Effects of ultrasound guidance on the minimum effective anaesthetic volume required to block the femoral nerve. *Br J Anaesth, 98*(6), 823-827. doi: 10.1093/bja/aem100

Chan, Candice, Lam, Felix, & Rohling, Robert. (2005). A needle tracking device for ultrasound guided percutaneous procedures. *Ultrasound in medicine & biology, 31*(11), 1469-1483.

Chan, Vincent WS, Nova, Hugo, Abbas, Sherif, McCartney, Colin JL, & Perlas, Anahi. (2006). Ultrasound examination and localization of the sciatic nerve: a volunteer study. *Anesthesiology, 104*(2), 309-314.

Chan, VincentW S., Perlas, Anahi, McCartney, ColinJ L., Brull, Richard, Xu, Daquan, & Abbas, Sherif. (2007). Ultrasound guidance improves success rate of axillary brachial plexus block. *Canadian Journal of Anesthesia, 54*(3), 176-182. doi: 10.1007/BF03022637

Cheng, HD, Shan, Juan, Ju, Wen, Guo, Yanhui, & Zhang, Ling. (2010). Automated breast cancer detection and classification using ultrasound images: A survey. *Pattern Recognition, 43*(1), 299-317.

Chin, Ki Jinn, & Chan, Vincent. (2008). Ultrasound-guided peripheral nerve blockade. *Current Opinion in Anesthesiology, 21*(5), 624-631.

Chin, Ki Jinn, Perlas, Anahi, Chan, Vincent WS, & Brull, Richard. (2008). Needle visualization in ultrasound-guided regional anesthesia: challenges and solutions. *Regional anesthesia and pain medicine, 33*(6), 532-544.

Choquet, Olivier, Abbal, Bertrand, & Capdevila, Xavier. (2013). The new technological trends in ultrasound-guided regional anesthesia. *Current Opinion in Anesthesiology, 26*(5), 605-612.

Czerwinski, Richard N, Jones, Douglas L, & O'Brien, WD. (1995). *Ultrasound speckle reduction by directional median filtering.* Paper presented at the Image Processing, 1995. Proceedings., International Conference on.

Falyar, C. R. (2010). Ultrasound in anesthesia: applying scientific principles to clinical practice. *AANA J, 78*(4), 332-340.

Gray, Andrew T. (2006). Ultrasound-guided Regional Anesthesia: Current State of the Art. *Anesthesiology, 104*(2), 368-373.

Gray, H. (1918). Gray's Anatomy of the Human Body. 20. from http://commons.wikimedia.org/wiki/File:Gray832.png

Gupta, Savita, Chauhan, RC, & Sexana, SC. (2004). Wavelet-based statistical approach for speckle reduction in medical ultrasound images. *Medical and Biological Engineering and computing, 42*(2), 189-192.

Hangiandreou, Nicholas J. (2003). AAPM/RSNA Physics Tutorial for Residents: Topics in US: B-mode US: Basic Concepts and New Technology 1. *Radiographics, 23*(4), 1019-1033.

Hannaford, Blake, Rosen, Jacob, Friedman, Diana W, King, Hawkeye, Roan, Phillip, Cheng, Lei, . . . White, Lee. (2013). Raven-II: an open platform for surgical robotics research. *Biomedical Engineering, IEEE Transactions on, 60*(4), 954-959.

Hargett, Mary Jean, Beckman, James D, Liguori, Gregory A, & Neal, Joseph M. (2005). Guidelines for regional anesthesia fellowship training. *Regional anesthesia and pain medicine, 30*(3), 218-225.

Hemmerling, T. M., Taddei, R., Wehbe, M., Cyr, S., Zaouter, C., & Morse, J. (2013). First Robotic Ultrasound-Guided Nerve Blocks in Humans Using the Magellan System. *Anesth Analg.* doi: 10.1213/ANE.0b013e3182713b49

Hemmerling, Thomas M, Taddei, Riccardo, Wehbe, Mohamad, Cyr, Shantale, Zaouter, Cedrick, & Morse, Joshua. (2013). First robotic ultrasound-guided nerve blocks in humans using the Magellan system. *Anesthesia & Analgesia, 116*(2), 491-494.

Hong, J, Dohi, Takeyoshi, Hashizume, Makoto, Konishi, K, & Hata, N. (2004). An ultrasound-driven needle-insertion robot for percutaneous cholecystostomy. *Physics in Medicine and Biology, 49*(3), 441.

Kapral, Stephan, Greher, Manfred, Huber, Gudrun, Willschke, Harald, Kettner, Stephan, Kdolsky, Richard, & Marhofer, Peter. (2008). Ultrasonographic guidance improves the success rate of interscalene brachial plexus blockade. *Regional anesthesia and pain medicine, 33*(3), 253-258.

Koscielniak-Nielsen, Z. J. (2008). Ultrasound-guided peripheral nerve blocks: What are the benefits? *Acta Anaesthesiologica Scandinavica, 52*(6), 727-737. doi: 10.1111/j.1399-6576.2008.01666.x

Loizou, Christos P, Pattichis, Constantinos S, Christodoulou, Christodoulos I, Istepanian, Robert SH, Pantziaris, Marios, & Nicolaides, Andrew. (2005). Comparative evaluation of despeckle filtering in ultrasound imaging of the carotid artery. *Ultrasonics, Ferroelectrics and Frequency Control, IEEE Transactions on, 52*(10), 1653-1669.

M. Jakopec, F. R. Baena, S. J. Harris, P. Gomes, J. Cobb, and B. L. Davies. (2003). The hands-on orthopaedic robot acrobot: Early clinical trials of total knee replacement surgery. *IEEE Trans. Robot. Autom., 19*(5), 9.

Marhofer, P, Sitzwohl, C, Greher, M, & Kapral, S. (2004). Ultrasound guidance for infraclavicular brachial plexus anaesthesia in children. *Anaesthesia, 59*(7), 642-646.

Marhofer, P., Greher, M., & Kapral, S. (2005). Ultrasound guidance in regional anaesthesia. *British Journal of Anaesthesia, 94*(1), 7-17. doi: 10.1093/bja/aei002

Mateo, Juan L, & Fernández-Caballero, Antonio. (2009). Finding out general tendencies in speckle noise reduction in ultrasound images. *Expert Systems with Applications, 36*(4), 7786-7797.

Morse, J, Terrasini, N, Wehbe, M, Philippona, C, Zaouter, C, Cyr, S, & Hemmerling, TM. (2014). Comparison of success rates, learning curves, and inter-subject performance variability of robot-assisted and manual ultrasound-guided nerve block needle guidance in simulation. *British Journal of Anaesthesia, 112*(6), 1092-1097.

Morse, Joshua, Wehbe, Mohamad, Taddei, Riccardo, Cyr, Shantale, & Hemmerling, Thomas M. (2013). Magellan: technical description of a new system for robot-assisted nerve blocks. *Journal of Computers, 8*(6), 1401-1405.

Narouze, S. N., Provenzano, D., Peng, P., Eichenberger, U., Lee, S. C., Nicholls, B., & Moriggl, B. (2012). The American Society of Regional Anesthesia and Pain Medicine, the European Society of Regional Anaesthesia and Pain Therapy, and the Asian Australasian Federation of Pain Societies Joint Committee recommendations for education and training in ultrasound-guided interventional pain procedures. *Reg Anesth Pain Med, 37*(6), 657-664. doi: 10.1097/AAP.0b013e318269c189

Neal, Joseph M. (2010). Ultrasound-guided regional anesthesia and patient safety: an evidence-based analysis. *Regional anesthesia and pain medicine, 35*(2), S59-S67.

Nixon, Mark. (2008). *Feature extraction & image processing*: Academic Press.

Norman, Donald A. (2002). *The design of everyday things*: Basic books.

Norman, Donald A, & Draper, Stephen W. (1986). User centered system design. *New Perspectives on Human-Computer Interaction, L. Erlbaum Associates Inc., Hillsdale, NJ.*

Nowakowski, P., Bierylo, A., Duniec, L., Kosson, D., & Lazowski, T. (2013). The substantial impact of ultrasound-guided regional anaesthesia on the clinical practice of peripheral nerve blocks. *Anaesthesiol Intensive Ther, 45*(4), 223-229. doi: 10.5603/AIT.2013.0043

NYSORA, New York School of Regional Anesthesia. (2013, 20/09/2013). Ultrasound-Guided Popliteal Sciatic Block. from http://www.nysora.com/techniques/ultrasound-guided_techniques/lower-extremity/3418-ultrasound-guided-popliteal-sciatic-block.html

Orebaugh, S. L., Bigeleisen, P. E., & Kentor, M. L. (2009). Impact of a regional anesthesia rotation on ultrasonographic identification of anatomic structures by anesthesiology residents. *Acta Anaesthesiol Scand, 53*(3), 364-368. doi: 10.1111/j.1399-6576.2008.01862.x

Perlas, Anahi, Brull, Richard, Chan, Vincent WS, McCartney, Colin JL, Nuica, Alina, & Abbas, Sherif. (2008). Ultrasound guidance improves the success of sciatic nerve block at the popliteal fossa. *Regional anesthesia and pain medicine, 33*(3), 259-265.

Pizurica, Aleksandra, Philips, Wilfried, Lemahieu, Ignace, & Acheroy, Marc. (2003). A versatile wavelet domain noise filtration technique for medical imaging. *Medical Imaging, IEEE Transactions on, 22*(3), 323-331.

Portnoy, Felix, & Milgram, Paul. (2008). The Effect of Low-Pass Filtering on Target Detection in Simulated Ultrasound Images. *Proceedings of the Human Factors and Ergonomics Society Annual Meeting, 52*(18), 1272-1276. doi: 10.1177/154193120805201825

Portnoy, Felix, Milgram, Paul, & McCartney, Colin J. (2008). The Use of Low-Pass Image Filtering to Facilitate Detection of Peripheral Nerves for Ultrasound-Guided Nerve Block Procedures. *Proceedings of the Human Factors and Ergonomics Society Annual Meeting, 52*(12), 898-902. doi: 10.1177/154193120805201229

R. H. Taylor, L. Joskowicz, B. Williamson, A. Gueziec, A. Kalvin, P. Kazanzides, R. V. Vorhis, J. Yao, R. Kumar, A. Bzostek et al. (1999). Computer-integrated revision total hip replacement surgery: Concept and preliminary results. *Med. Imag. Anal., 3*(3), 19.

Rotemberg, V., Palmeri, M., Rosenzweig, S., Grant, S., Macleod, D., & Nightingale, K. (2011). Acoustic Radiation Force Impulse (ARFI) imaging-based needle visualization. *Ultrason Imaging, 33*(1), 1-16.

Ruggiero, C, Bagnoli, F, Sacile, R, Calabrese, M, Rescinito, G, & Sardanelli, F. (1998). *Automatic recognition of malignant lesions in ultrasound images by artificial neural networks.* Paper presented at the Engineering in Medicine and Biology Society, 1998. Proceedings of the 20th Annual International Conference of the IEEE.

S. Horgan, C. Galvani, M. V. Gorodner, P. Omelanczuck, F. Elli, F. Moser, L. Durand, M. Caracoche, J. Nefa, S. Bustos et al. (2005). Robotic-assisted heller myotomy versus laparoscopic heller myotomy for the treatment of esophageal achalasia: Multicenter study,. *J. Gastroint. Surg., 9*(8), 10.

S. J. Marecik, V. Chaudhry, A. Jan, R.K Pearl, J. J. Park, and L. M. Prasad. (2007). A comparison of robotic, laparoscopic, and hand-sewn intestinal sutured anastomoses performed by residents. *American Journal of Surgery, 193*(3), 6.

Sandhu, NS, & Capan, LM. (2002). Ultrasound−guided infraclavicular brachial plexus block. *British Journal of Anaesthesia, 89*(2), 254-259.

Schafhalter-Zoppoth, Ingeborg, McCulloch, Charles E, & Gray, Andrew T. (2004). Ultrasound visibility of needles used for regional nerve block: an in vitro study. *Regional anesthesia and pain medicine, 29*(5), 480-488.

Shi, Jiaxi, Schwaiger, Johannes, & Lueth, Tim C. (2011). *Nerve block using a navigation system and ultrasound imaging for regional anesthesia.* Paper presented at the Engineering in Medicine and Biology Society, EMBC, 2011 Annual International Conference of the IEEE.

Sinha, Avinash, & Chan, Vincent WS. (2004). Ultrasound imaging for popliteal sciatic nerve block. *Regional anesthesia and pain medicine, 29*(2), 130-134.

Sites, B. D., Gallagher, J. D., Cravero, J., Lundberg, J., & Blike, G. (2004). The learning curve associated with a simulated ultrasound-guided interventional task by inexperienced anesthesia residents. *Reg Anesth Pain Med, 29*(6), 544-548.

Sites, B. D., Spence, B. C., Gallagher, J. D., Wiley, C. W., Bertrand, M. L., & Blike, G. T. (2007). Characterizing novice behavior associated with learning ultrasound-guided peripheral regional anesthesia. *Reg Anesth Pain Med, 32*(2), 107-115. doi: 10.1016/j.rapm.2006.11.006

Sites, Brian D, Gallagher, John D, Cravero, Joseph, Lundberg, Johan, & Blike, George. (2004). The learning curve associated with a simulated ultrasound-guided interventional task by inexperienced anesthesia residents. *Regional anesthesia and pain medicine, 29*(6), 544-548.

Sonosite. (2013). Sonosite X-Porte Product Gallery. from http://www.sonosite.com/products/x-porte

Sviggum, H. P., Ahn, K., Dilger, J. A., & Smith, H. M. (2013). Needle echogenicity in sonographically guided regional anesthesia: blinded comparison of 4 enhanced needles and validation of visual criteria for evaluation. *J Ultrasound Med, 32*(1), 143-148.

Takatani, J., Takeshima, N., Okuda, K., Uchino, T., Hagiwara, S., & Noguchi, T. (2012). Enhanced Needle Visualization: advantages and indications of an ultrasound software package. *Anaesth Intensive Care, 40*(5), 856-860.

Taxt, Torfinn. (1995). Restoration of medical ultrasound images using two-dimensional homomorphic deconvolution. *Ultrasonics, Ferroelectrics and Frequency Control, IEEE Transactions on, 42*(4), 543-554.

Taxt, Torfinn, & Strand, Jarle. (2001). Two-dimensional noise-robust blind deconvolution of ultrasound images. *Ultrasonics, Ferroelectrics and Frequency Control, IEEE Transactions on, 48*(4), 861-866.

Tony F. Chan, Luminita A. Vese. (2001). Active Contours Without Edges. *IEEE TRANSACTIONS ON IMAGE PROCESSING, 10*(2), 12.

Tsui, B. C., & Finucane, B. T. (2006). The importance of ultrasound landmarks: a "traceback" approach using the popliteal blood vessels for identification of the sciatic nerve. *Reg Anesth Pain Med, 31*(5), 481-482. doi: 10.1016/j.rapm.2006.03.008

Vilchis, Adriana, Troccaz, Jocelyne, Cinquin, Philippe, Masuda, Kohji, & Pellissier, Franck. (2003). A new robot architecture for tele-echography. *Robotics and Automation, IEEE Transactions on, 19*(5), 922-926.

Vloka, Jerry D., Hadžic, Admir, April, Ernest, & Thys, Daniel M. (2001). The Division of the Sciatic Nerve in the Popliteal Fossa: Anatomical Implications for Popliteal Nerve Blockade. *Anesthesia & Analgesia, 92*(1), 215-217 210.1097/00000539-200101000-200100041.

Vloka, Jerry D., Hadžic, Admir, Kitain, Eric, Lesser, Jonathan B., Kuroda, Max, April, Ernest W., & Thys, Daniel M. (1996). Anatomic Considerations for Sciatic Nerve Block in the Popliteal Fossa Through the Lateral Approach. *Regional anesthesia and pain medicine, 21*(5), 414-418.

Yue, Yong, Croitoru, Mihai M, Bidani, Akhil, Zwischenberger, Joseph B, & Clark, John W. (2006). Nonlinear multiscale wavelet diffusion for speckle suppression and edge enhancement in ultrasound images. *Medical Imaging, IEEE Transactions on, 25*(3), 297-311.